



**Politecnico  
di Torino**

Politecnico di Torino

**Master of Science in Automotive Engineering**

Master Thesis

**Refinement of a Matlab tool for combustion analysis applied to CI  
engines running with conventional diesel fuel and HVO**

**Supervisors:**

Prof. Stefano D'Ambrosio  
Prof. Roberto Finesso

**Candidate:**

Filippo Pizzo

December 2021



## Sommario

<b>Abstract</b> .....	<b>5</b>
<b>Introduction</b> .....	<b>6</b>
<b>1. Compression ignition engines</b> .....	<b>8</b>
1.1. Diesel cycle and general overview .....	8
1.2. Combustion process .....	12
1.3. Characteristic pollutant of a compression ignition engine: NO <sub>x</sub> and PM .....	16
1.4. Renewable fuel: HVO .....	23
<b>2. General information about the tool</b> .....	<b>24</b>
<b>3. One zone model</b> .....	<b>29</b>
3.1. Trapped mass and mean temperature estimation .....	29
3.2. SOC estimation and Heat Release Rate curve .....	31
3.3. End of combustion (EOC) .....	34
3.4. Mass fraction burned and combustion metrics .....	34
<b>4. Three zone model</b> .....	<b>42</b>
4.1. Injection profile .....	47
4.2. Model calibration .....	49
4.3. Graphical result .....	52
4.4. Comparison between Diesel and HVO .....	57
4.5. Comparison between one zone and three zone model.....	60
4.6. EGR effects .....	66
<b>5. Submodel for NO<sub>x</sub> formation</b> .....	<b>69</b>
<b>6. Submodel for PM formation</b> .....	<b>76</b>
<b>7. Conclusions</b> .....	<b>82</b>
<b>Bibliography</b> .....	<b>83</b>



## Abstract

This project has the aim of refining an existing zero-dimensional diagnostic tool developed in Matlab environment in order to analyse the combustion process of a compression ignition engine. The engine under exam is the F1A engine (FPT Industrial), a turbocharged diesel engine with a displacement of 2.3 litres. In addition to the common diesel fuel, a renewable fuel was also used (HVO) in order to evaluate what benefits could be achieved using this type of new fuel. Two models were used inside the tool: a complete one zone model and a three zone model, that is also used in order to evaluate the evolution of particulate matter (PM) and nitrogen oxides (NO<sub>x</sub>) emissions as function of the crank angle. The investigated injection strategy has two pilot injections and a main one (ppM injection strategy) at three key points (1250x2, 2000x8.96 and 2250x15), with different EGR rates.

## Introduction

Until today the internal combustion engine has played a very important role in the transportation sector. The reason of its widespread use has to be searched on its peculiar feature: its architecture is relatively simple (if compared, for example, to the first steam engines used for transportation) and the fuel that are used to run it (gasoline, diesel or LPG) have an higher energy density if compared with other propulsion solutions (electric vehicles or fuel cell vehicles). But it also has some disadvantages:

- Conventional fuels are fossil fuels and they are a non-renewable source of energy. The demand of such energy source is constantly increasing, so in the next future the demand could not be satisfied.
- The efficiency of the cycle is not so great (it is in the order of 30/35%).
- Fuel combustion is not an ideal process and it leads to formation of some pollutant species, such as carbon dioxide (CO<sub>2</sub>), nitrogen oxides (NO<sub>x</sub>), unburned hydrocarbons (HC) and particulate matter (PM, especially for what regards combustion in diesel engines). This pollutant substances are not good for human health and for the environmental one (for example, CO<sub>2</sub> emissions contribute to the Greenhouse Effect).

This last reason leads government agencies around the world to put some limits on the pollutant emission. For example, nowadays the homologation rules set a limit of 95g/km for the CO<sub>2</sub> emission (calculated on the average of the fleet). This limits are quite challenging for the OEMs and they have pushed the research for new devices aimed to bring them inside the limits. The ideal solution would be full-electrified powertrains, since they are pollutant-free (if we are considering Tank-to-Wheel emissions), but nowadays there are some problems, such as the allowable range, the number of the charging stations and the time to recharge batteries. So, constructors are pushing for continuously improving the internal combustion engines with new injection strategies (from 'Unijet' to multi-injection strategies) and new aftertreatment devices (EGR, SCR or particulate filters).

This work has the aim of refine a zero dimensional Matlab tool for combustion and pollutant emission analysis in order to adapt it to a new type of engine and to make some consideration on the usage of alternative fuels, such as HVO.

The first chapter gives a general overview on the compression ignition engines, such as the thermodynamic cycle and principal features.

Then it is analysed the injection system, the combustion process according to the Dec's theory and an overview on the formation mechanism of nitrogen oxides and particulate matter is done.

The second chapter gives some information about the combustion models there are used in this work, some information about the engine and fuels that are used, the method used to calculate the absolute pressure inside the cylinder and the filtering technique.

The third chapter deals with the one zone model, introducing the parameters used to analyse the combustion process, such as heat release rate, gross heat transfer and mass fraction burned curve.

The fourth chapter describe the thermodynamic equations that are behind the three zone model. The scheme is similar to the one of the one zone, with a focus on the construction of the injection profile.

The last chapters are focused on the modelling of the formation mechanism of nitrogen oxides and particulate matter and an analysis of the influence of EGR on combustion parameters and emission is done.

# 1. Compression ignition engines

## 1.1. Diesel cycle and general overview

Compression ignition engines have as thermodynamic reference model the diesel cycle. This cycle is made by two adiabatic transformation (that represent the intake and the expansion strokes), a constant pressure heating (that represents the combustion phase) and a constant volume reject of heat (the exhaust phase). These two last transformation are used since the cycle considers only air as fluid.

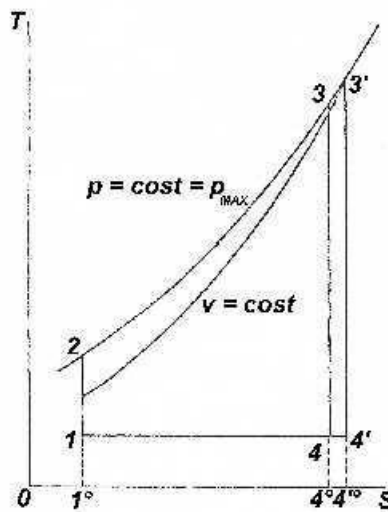


Figure 1. Errore. Nel documento non esiste testo dello stile specificato..1 T-S diagram of the diesel cycle

The reason why the heat addition occurs on a constant pressure phase and not in a constant volume phase could be found looking at the *Figure 1.1*. In fact, with the same amount of heat introduced in the cycle, if the heat addition would be done at constant volume, the fluid inside the cycle will reach higher temperature, which means higher heat that is rejected to the external environment, and so a lower efficiency of the cycle (look at the area  $1^{\circ}144^{\circ}$  and  $1^{\circ}14'4^{\circ}$ ).

In compression ignition engines it is not needed the presence of a spark (like in gasoline engines) to start the combustion, but it starts thanks to the 'autoignition' of the mixture. In order to obtain the autoignition we need an high-reactivity fuel, such as diesel or 'sustainable' diesels. The fuels used are long-chain molecules, that are more flexible than short-chain fuels, and so the reactions that lead to the combustion process are faster.

Since the fuel is highly reactive, it is not possible to mix it with air during the intake stroke (like it is done with spark ignition engines), but it has to be injected directly inside the cylinder (or in a prechamber, if old-technology diesel engines are examined) toward the end of the compression stroke, where temperature and pressure

are high (about 900 K and 30-40 bar) and there are the conditions are good for the autoignition.

The fuel is injected at very high pressure (with modern Common Rail systems it is possible to reach maximum injection pressure greater than 2000 bar), so that the fuel is injected as a spray of microscopic droplets, in order to make easier the mixing process between the fuel and the surrounding compressed air. It is important to keep in mind that the mixing is not homogeneous like in spark ignition engines, but it is highly heterogeneous. The global combustion process is made with a lean mixture (there is an excess of oxygen with respect the stoichiometric value) but, for example, in the region near the injector tip the mixture it is possible to see region of rich mixture. Thanks to the high reactivity of the fuel, these rich region will burn, but the lack of oxygen will lead to the formation of carbonaceous residuals that will contribute to the emission of particulate matter.

An important advantage of compression ignition engines with respect spark ignition ones is the absence of the throttle valve. In fact, in order to regulate the load of a diesel engine, is sufficient to regulate the quantity of fuel that is injected. The absence of the throttle valve leads to an improvement of the efficiency of the engine at partial loads, since the pumping work is highly reduced. A drawback with respect spark ignition engines could be found on the maximum rotational speed. In fact, when the engine speed increases, the time required for the combustion process slightly decreases, but not in such a way to compensate the increase of the engine speed. This means that the angular duration of the combustion is increasing with the engine speed [1]. In order to limit the angular combustion duration, the maximum engine speed is limited to about 5000 rpm.

Another distinctive property of compression ignition engines is also the combustion noise. When the fuel is injected inside the cylinder, it requires a certain amount of time to vaporize and then the combustion process starts. So, there is a fuel accumulation inside the cylinder and the greater this fuel accumulation the steeper is the increasing of the in-cylinder pressure. This phenomenon causes the vibration of the engine walls, that produce the characteristic sound of the old diesel engines. Nowadays this phenomenon is mitigated using one or more pilot injections (few percentage of the total fuel injected over the cycle) in order to initiate the combustion process when the main injection starts.

Modern diesel engines are equipped with an electromagnetic injection systems, that is called '*Common Rail*' (CR). The CR systems has completely substitute the old mechanical injection system because of higher injection pressure (so, better fuel atomization) and because it allows an higher number of possible injection strategies. The schematic of a CR system could be seen in the *Figure 1.2* [2].

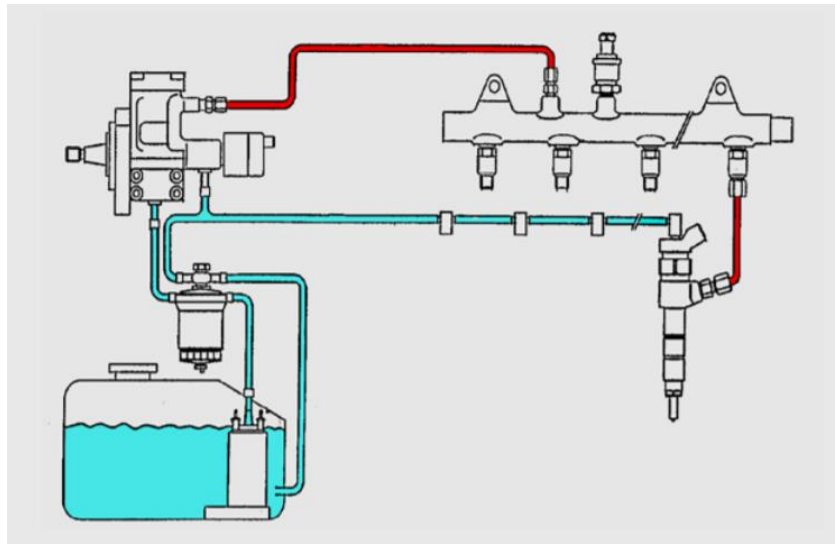


Figure 1.2 Common Rail layout

In the above figure, the cyan line is the low pressure line, while the red line is the high pressure line. The fuel is drawn from the tank thanks to the low pressure pump, that sends it to the fuel filter and then to the high pressure pump, that takes the fuel pressure up to 2000 bar. Then the fuel is sent to the common rail, that feeds the fuel injectors. The pressure inside the fuel rail is adjusted by means of a pressure regulation valve, that sends the excess flow of fuel back to the tank.

The most sophisticated component of the fuel injection system is the injector. In the solenoidal acting injector, the injector is opened by means of a current that flows through a solenoid. A schematic sketch of a solenoidal injector for compression ignition engines is reported in the *Figure 1.3* [1].

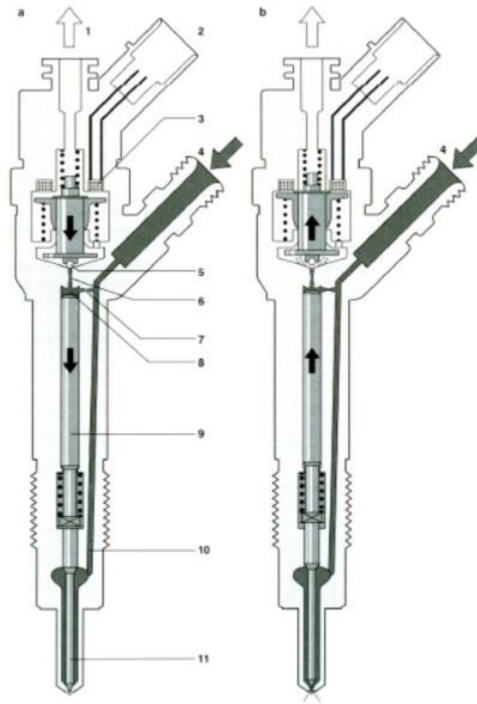


Figure 1.3 Common rail solenoidal injector

The force required to open the nozzle are very high, and so, if we want to open the injector just using the solenoidal acting, a very big solenoid is needed. This problem is resolved using indirect acting injectors. In fact, the solenoid does not open acts directly on the pushrod, but it acts on a pilot stage.

From the above sketch, it is possible to see that the fuel acts both on the upper part (the so called *control chamber*) and on the lower part of the pushrod. Since the upper area is bigger than the lower one, the injector is maintained in normally closed position simply by the fuel pressure. When a current excites the solenoid, the control chamber is connected to a low pressure environment (the low pressure side of the fuel pump) by means of a calibrated orifice. This connection with a low pressure environment reduces the pressure on the upper side of the pushrod, so the injector is rapidly opened.

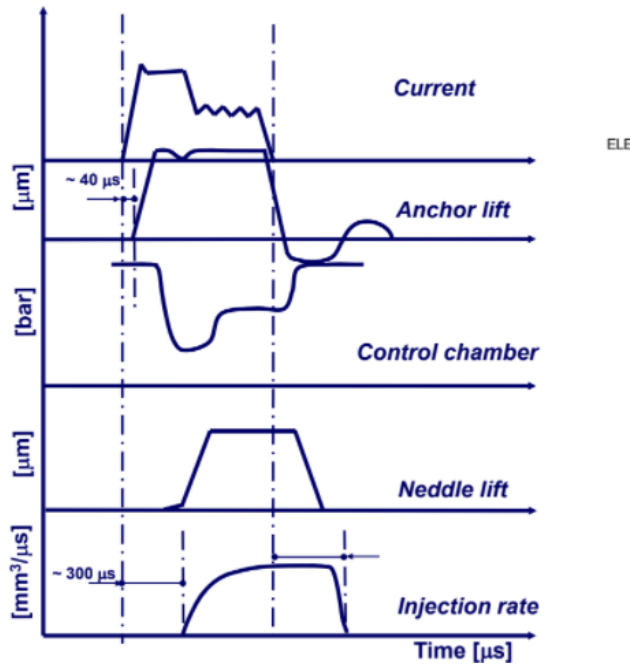


Figure 1.4 Time evolution of injector parameters

In the *Figure 1.4* [1] it is possible to see the time evolution of some of the working parameters of a indirect acting solenoidal injector. Looking at the anchor lift curve, there is a delay between the anchor lift and the current signal (when the current starts to become greater than 0 there is the so called *electric start of injection* ( $SOI_{el}$ )). This is due to the fact that the current needs to be higher than a certain value  $I_0$  to open the control volume connecting channel. Another delay is due to two factors: when the control chamber is connected with the low pressure environment, the pressure does not drop instantaneously, but it takes some time, since the orifice diameter is very small. Moreover, the needle has to recover some elastic deformations that occurs when it is closed (looking at the last two curves of the above figure, it is possible to see that a certain needle lift is required to start the hydraulic injection). All this delays are condensed in the so called *Nozzle Opening Delay* (NOD).

A similar delay occurs also during the closing phase. In fact, since the current is higher than  $I_0$  the solenoid is lifting up the anchor, so the injector is in open position. When the anchor reaches its seats, the pressure in the control volume has to rise up to the fuel pressure, in order to close the injector. The sum of these two delays (electrical and hydraulic) is the *Nozzle Closing Delay* (NCD). This two delays are strictly dependent of the type of injector that are used.

## 1.2. Combustion process

The combustion process of a compression ignition engine could be summarized using the *Figure 1.5* [3], that subdivide the entire process into four parts:

- The ignition delay (AB);
- The premixed phase (BC);
- The mixing-controlled phase (CD);
- The late combustion phase (DE);

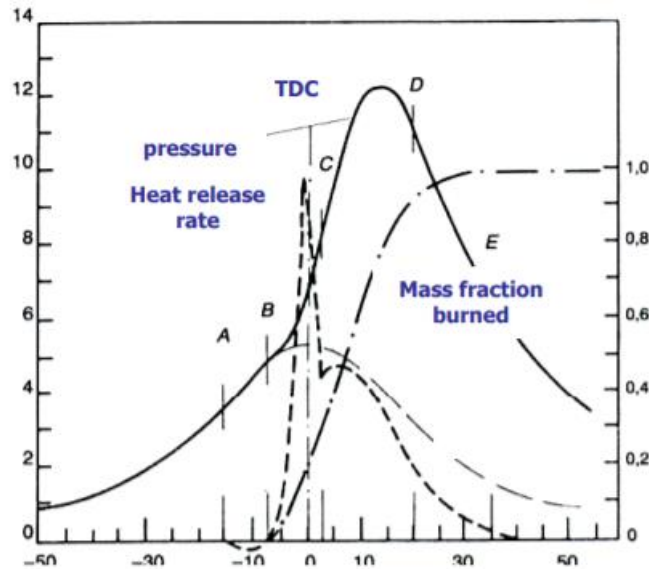


Figure 1.5 Heat release, pressure and mass fraction burned for a CI engine

The point A is the starting point of the hydraulic injection of the fuel, and the in-cylinder pressure follows the motored one (constructed using polytropic transformations) until the point B, that is the start of combustion crank angle (SOC). In fact, the fuel is not burning instantaneously when it is injected inside the combustion chamber. This is because there are both physical and chemical phenomena. The first ones are the vaporization of the fuel and the mixing with the air, while the second ones are the intermediate reactions that leads to the exothermic transformation (but these last phenomena are negligible in a compression ignition engine, since the fuel used is an high reactivity one). During this interval, the fuel is accumulating inside the combustion chamber.

When the first particles starts to burn (point B), the temperature increases suddenly and all the fuel that was accumulated burns instantaneously, causing the steep increase of the in-cylinder pressure. This steep increase of the pressure is responsible of the typical combustion noise of the compression ignition engine, but it is good for what regard the combustion efficiency (the peak of the heat release rate curve is in the neighbored of the TDC. The fuel that burns under the premixed phase is a small part of the total fuel that is injected (around 10%).

When the accumulated fuel is consumed, the heat release rate depends on the rate at which new fuel particles are allowable for combustion. In other words, the heat

release curve depends on the injection rate. A challenging point in this interval is to have sufficient oxygen to burn the injected fuel, since there is an always increasing percentage of burned gas in the cylinder. So, this is the phase in which the greatest part of soot is generated. Normally, this is also the phase in which it is possible to find the peak pressure of the cycle.

The late combustion phase is the phase in which the reactions slowly decrease their rate and in which a partial oxidation of the soot formed in the previous phase could happen. It is important that the length of this interval is limited, since the piston is gradually going away from the TDC.

There are some conceptual models used to describe combustion phenomena for a compression ignition engine, but the most used is the one that was proposed by John Dec in 1997. The engine used by Dec was a special engine, with some optical accesses and a laser sheet. A schematic view of the optical-access engine is reported below in the *Figure 1.6* [4].

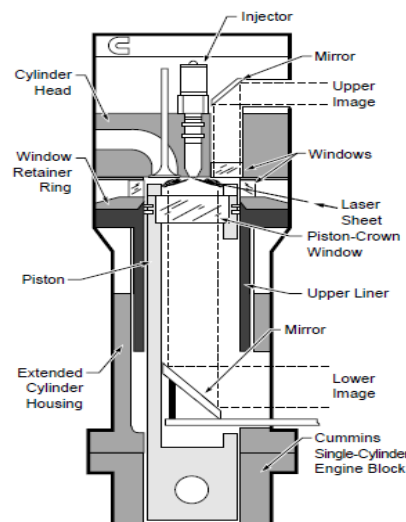


*Figure 1.6 Optical-access engine*

Thanks to these changes it is possible to see the penetration of the liquid jet, the atomization of the fuel and the interaction of the fuel with the surrounding air, in order to better analyse the evolution of the combustion process. The evolution of the fuel jet and conditions inside the cylinder are reported in the *Figure 1.7* [4].

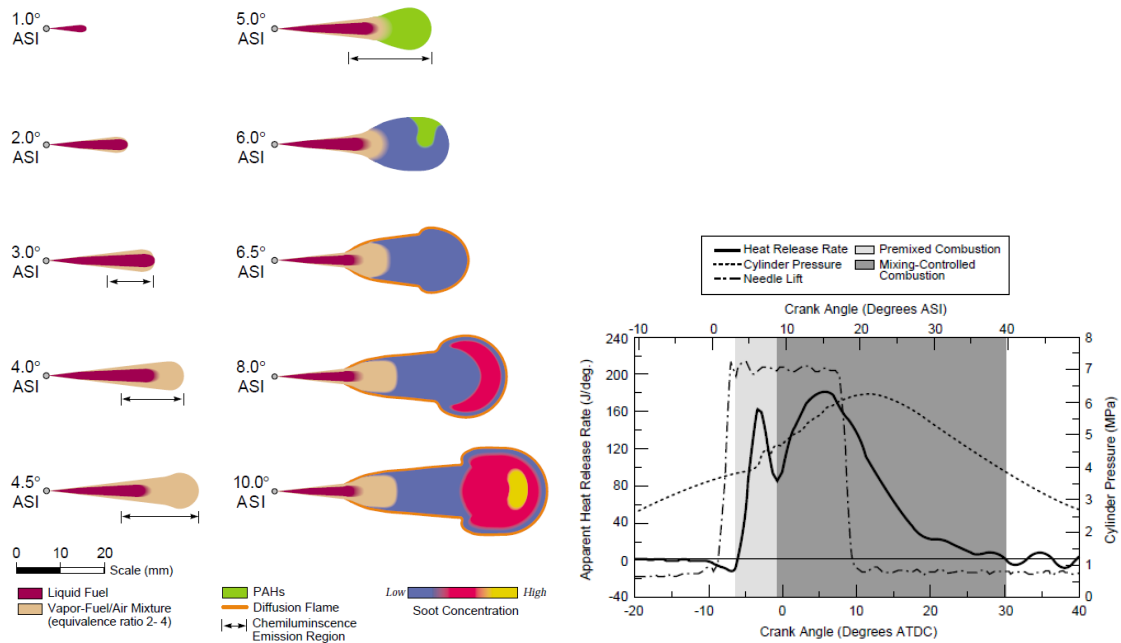


Figure 1.7 Dec's jet evolution model (on the left) and apparent heat release, needle lift and pressure signal (on the right)

From the figure above, it is possible to see that  $1^\circ$  after the start of injection the fuel jet is only formed by the liquid fuel. After another degree, a vapor-fuel region starts to be visible in a region alongside the liquid jet, that continues to advance inside the cylinder. At  $3^\circ$  ASI the liquid jet reaches its maximum liquid length and some chemiluminescence starts to be visible. At  $4^\circ$  ASI the vapor-fuel region continues to become bigger and bigger and there is an increasing of the luminescence emitted. Looking at the AHRR trace on the figure, at this point seems to start the premixed phase of the combustion. At  $4.5^\circ$  ASI it could be noticed a zone of rich vapor-fuel/air mixture (the equivalence ratio is about 2-4) behind the liquid jet. At  $5^\circ$  the first particles of PAHs (Polycyclic Aromatic Hydrocarbons) starts to be visible. This particles could react in an environment with a low oxygen concentration (so rich mixture) also when the temperature are not so high. At  $6^\circ$  ASI it is possible to see the first particles of soot that are formed and the diffusive flame starts to develop. At  $6.5^\circ$  ASI the thin diffusive flame completely encircles the jet. At  $8^\circ$  ASI the premixed combustion is completely finished and it could be noticed an increasing concentration of soot at the head of the jet. At  $10^\circ$  ASI the concentration of soot is high on the head of the jet and lower on the periphery, since it is oxidized.

### 1.3. Characteristic pollutant of a compression ignition engine: $\text{NO}_x$ and PM

One of the critical aspects of an internal combustion engine is that at the exhaust we can not find only  $\text{CO}_2$  and  $\text{H}_2\text{O}$ , as expected looking at the combustion reaction. In fact, since the combustion efficiency is lower than the unit and thanks to secondary reactions that can occur in the combustion chamber or in exhaust line, at the exhaust of an internal combustion engine some pollutant species could be found. These pollutant species are seriously dangerous both for human life and for the environmental point of view. Speaking about compression ignition engines, the two pollutant species that this work is going to treat are nitrogen oxides ( $\text{NO}_x$ ) and particulate matter (PM).

For the analysis of the formation of  $\text{NO}_x$  two formation mechanisms are mainly used:

- Zeldovich mechanism (also known as thermal mechanism);
- Prompt mechanism;

The Zeldovich mechanism is composed by six reactions that involve atomic nitrogen that is present in the air breathed by the engine. The combustion process develops very high temperatures, that break the chemical bond between the nitrogen and the oxygen present in the air. In the burned gas region these two species bond together again, forming nitrogen oxides. The rate of formation of this pollutant species is not comparable with the combustion velocity, but its velocity increases exponentially with respect to the temperature inside the cylinder. So, in order to understand how the thermal mechanism works, we have to highlight the peak value of the temperature reached inside the cylinder and the oxygen concentration. The six equations of the thermal mechanism are reported below:

- 1)  $\text{N}_2 + \text{O} \rightarrow \text{NO} + \text{N}$
- 2)  $\text{N} + \text{O}_2 \rightarrow \text{NO} + \text{O}$
- 3)  $\text{N} + \text{OH} \rightarrow \text{NO} + \text{H}$
- 4)  $\text{H} + \text{N}_2\text{O} \rightarrow \text{N}_2 + \text{OH}$
- 5)  $\text{O} + \text{N}_2\text{O} \rightarrow \text{N}_2 + \text{O}_2$
- 6)  $\text{O} + \text{N}_2\text{O} \rightarrow \text{NO} + \text{NO}$

Since the mixture composition inside the combustion chamber is really heterogeneous, there will be a non-uniform temperature distribution inside the cylinder, and so a non-uniform formation process of nitrogen oxides. For example, in the premixed phase, where the equivalent air/fuel ratio is about 2-4, there is a lack of

oxygen, and so the formation rate of nitrogen oxides is very low. In the diffusive flame, on the contrary, the temperature are higher and the mixture is close to stoichiometric value, so there will be high rate of formation of these species. When the temperature falls down during the expansion stroke there is not the expected decomposition of NO, but the reaction is “frozen”, and so analysing the exhaust gases it is possible to find an higher concentration of nitrogen oxides than expected. One example of this “freezing” effect could be analysed looking at the ratio between the emission of NO<sub>2</sub> over the emission of NO. The concentration ratio of these two species is showed in the *Figure 1.8* [3] as function of the load and of the engine speed.

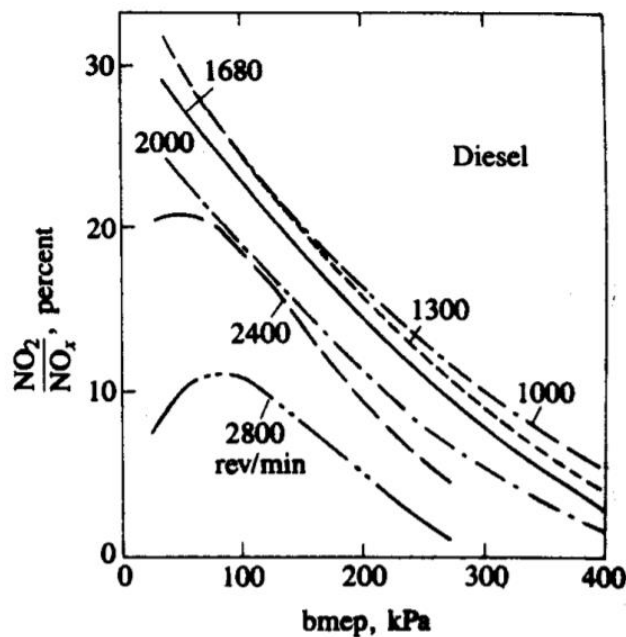
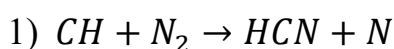


*Figure 1.8 NO<sub>2</sub>/NO ratio ad function of load and engine speed*

The chemical equilibrium of the exhaust gases and the diffusive flame temperature lead us to think that the concentration of NO<sub>2</sub> will be negligible with respect the NO one. But the sudden fall of the temperature inside the combustion chamber during the expansion stroke blocks the reactions that convert NO<sub>2</sub> into NO.

The second formation mechanism of NO<sub>x</sub> analysed is the prompt one. It is called “prompt” because it is a very fast process and it is influenced very poorly by the temperature in the cylinder. The two reactions that describe this mechanism are reported below:



In the prompt mechanism, the formation rate of the nitrogen oxides is promoted by the reaction of an hydrocarbon or a radical group with an atom of nitrogen (in the thermal mechanism the entire process was promoted by atoms of oxygen). Since the needing of the reaction of an hydrocarbon or a radical with the nitrogen, this mechanism is really valid in region of rich air/fuel mixture: for example, the radical CH is a typical radical of zones of incomplete combustion. The following graph will report the concentration of the nitrogen oxides obtained using this formation mechanism with respect the concentration obtained at the chemical equilibrium condition in the logarithmic scale as function of the equivalent air/fuel ratio.

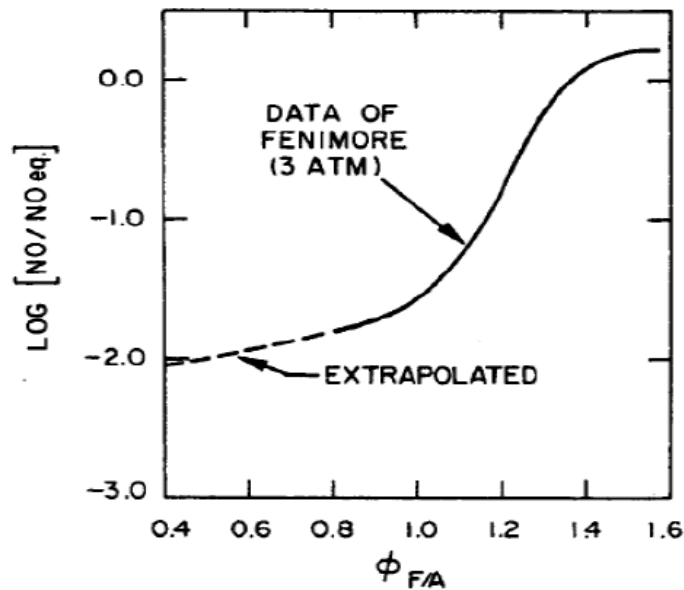


Figure 1.9 Ratio between "prompt" NO and the equilibrium one as function of the equivalent air/fuel ratio [7]

The main parameters that influence the quantity of nitrogen oxides present in the combustion chamber crank angle by crank angle are:

- EGR level
- Equivalent ratio (in other words, the load)
- Injection advance

The EGR level could influence strongly the level of nitrogen oxides into the cylinder. In fact, recirculating a percentage of the exhaust gases into the intake manifold allow to decrease the nitrogen oxides emission thanks to three effects:

- Dilution effect
- Thermic effect
- Chemical effect

The effect the most affects the nitrogen oxides level is the first one. In fact, if part of the exhaust gases are sent into the cylinder, they took space that although will be available for fresh air, so the oxygen concentration is decreased. The second effect exploits the fact that exhaust gases have an higher heat capacity with respect the fresh air, and so they are able to absorb a greater heat quantity, lowering the temperature inside the cylinder. The third effect is the one that influence in a minor part the nitrogen oxides emission and it exploits the dissociation reaction of the  $\text{CO}_2$  into  $\text{CO}$ , that is a reaction that absorbs heat, lowering the temperature.

Talking about the EGR level influence is a tricky matter. In fact, due to the fact the diesel engines are characterized by a global lean mixture, at the exhaust it is possible to find a certain quantity of oxygen that is higher at lower load. This means that the same EGR level produces different effects on the nitrogen oxides emission, depending on the engine load. So, what really matter for lowering the nitrogen oxides is not properly the EGR level, but the oxygen concentration in the intake manifold. The effects of EGR level and oxygen concentration are reported in the *Figure 1.10* [3].

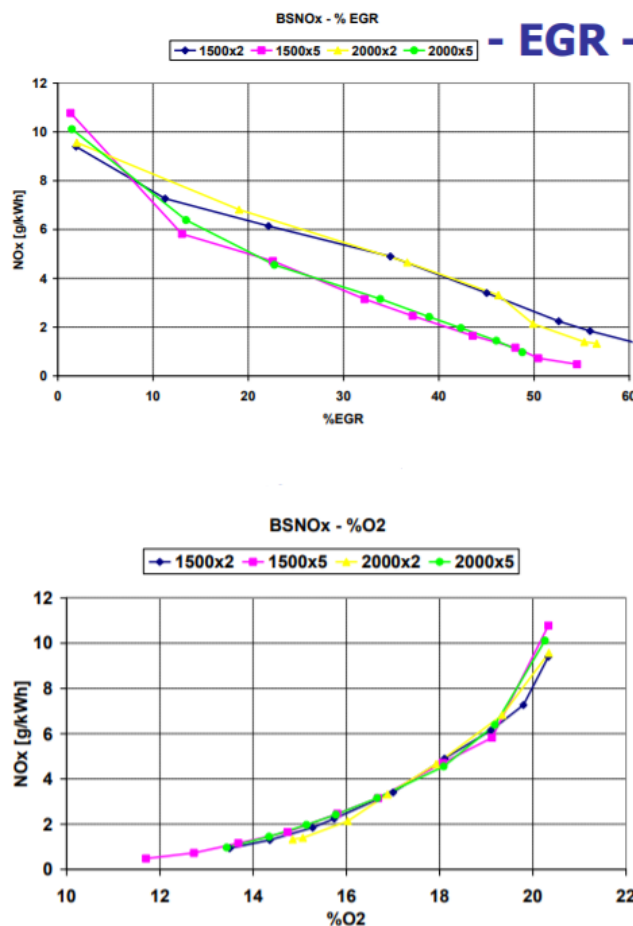


Figure 1.10 EGR level and oxygen concentration effects on NOx emission

For what regards the effects of the equivalent ratio, increasing the equivalent ratio (and so the engine load) means to increase nitrogen oxides formation, since pressure and temperature inside the cylinder are higher.

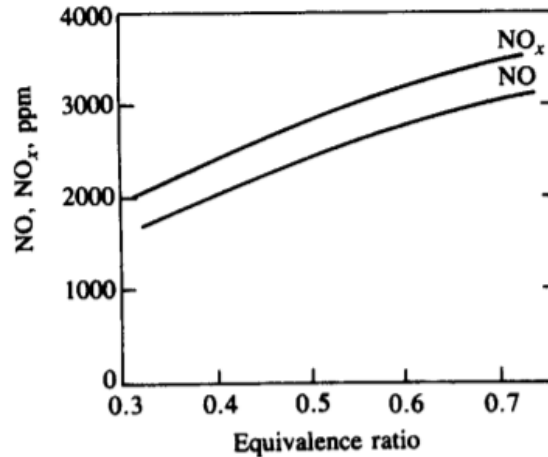


Figure 1.11 NO and NO<sub>x</sub> emission as function of the equivalent ratio [7]

It is interesting to note that lower the load does not influence too much on the nitrogen oxides emission, because the greatest part of the pollutant species is forming in the diffusive flame, where the air/fuel ratio is near to the stoichiometric one.

The last parameter that influence nitrogen oxides emission is the injection advance. Increasing the injection advance, since temperature and pressure are lower, more fuel is accumulating into the cylinder prior to start the combustion. So, when this fuel starts to burn all together during the premixed phase, there will be an higher peak in the heat release curve, that means the diffusive phase will be characterized by higher temperature, promoting the formation of nitrogen oxides.

For what regards particulate matter (**PM**), according to the regulation, it is defined as all the particles that are trapped by a specific filter that are coming out from the exhaust gas flow diluted in such a way to reach a temperature of 52°C. The definition is not defining any chemical molecule but only a mix of substances. The substances that are forming particulate matter are:

- Soluble organic fraction (SOF), that is organic material coming from fuel and lubricating oil
- Solid fraction, that are carbonaceous particles and ashes
- Sulphates (coming from the reaction of H<sub>2</sub>SO<sub>4</sub> with H<sub>2</sub>O)

The soluble fraction tend to decrease increasing the load: in this case the particulate matter tends to become “dry”. On the contrary, decreasing the load, the soluble

fraction increase and the particulate matter become “wet”. The SOF is formed by condensate hydrocarbons droplets or by hydrocarbons that are absorbed by the surface of some carbonaceous particles.

The solid fraction is composed by carbonaceous particles that form chemical bond with other elements. It is composed by hexagonal structures (called “platelets”) that join each other to form crystallite, that next will form the particles. The other part of the solid fraction is composed by ashes, in which it is possible to find some metal oxides that comes from liners, from the exhaust system or from some additives used in order to promote the regeneration of the particulate filter.

Particulate matter could be subdivided according to the aerodynamic diameter, that is the diameter of a sphere of unitary density that has the same deposit velocity of the particulate particles. The categories are:

- Nanoparticles, with an aerodynamic diameter lower than 50 nm
- Ultrafine particles, with a diameter lower than 0.1  $\mu\text{m}$
- Fine particles, with a diameter lower than 2.5  $\mu\text{m}$
- PM10 particles, with a diameter lower than 10  $\mu\text{m}$

Another subdivision that could be done is to divide particulate particles according to the composition and to the diameter. A graphical representation of this last subdivision is given in the *Figure 1.12* [3].

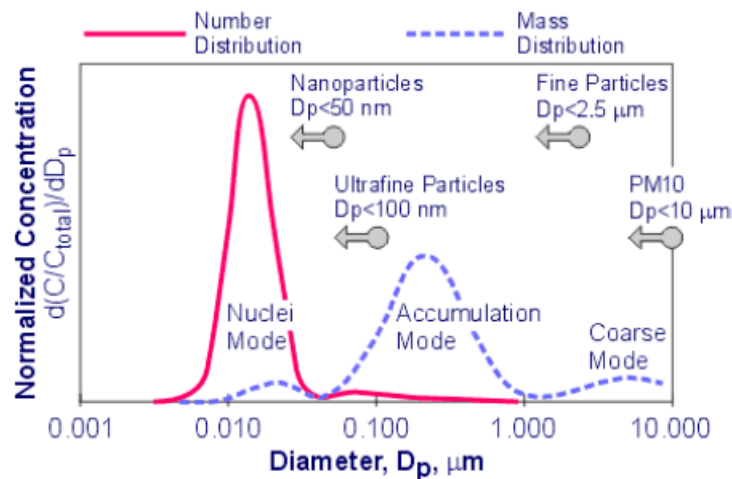


*Figure 1.12 Distribution of particulate matter particles*

- In the “Nuclei mode” there are nanoparticles that are mainly constituted by condensate sulphuric acid or hydrocarbons because the drop of temperature when the exhaust gases are diluted in the atmosphere or in the sampling bag during tests. From the above figure it is possible to see that these are the most

numerous particles category but, since their low aerodynamic diameter, they contribute poorly to the total mass of particulate matter emitted.

- In the “Accumulation mode” it is possible to find carbonaceous particles that absorb some hydrocarbons on their surface. The particles that are included in this category are ultrafine and fine particles. Their number is low, but their mass is quite high compared with other particles.
- The last category is the one of the “Coarse mode”, where are found particles with a diameter higher than 1  $\mu\text{m}$ . These particles are not a product of the combustion process, but they come from the liners and from the exhaust line. The number is very limited, but thanks to their greater diameter they represent the 15/20% of the total mass of PM.

The parameters that mainly affect PM emissions are:

- EGR level
- Engine load
- Injection advance

The EGR level influence particulate matter emission since the greatest the quantity of recirculated gases the lower the oxygen concentration in the cylinder. Limiting the oxygen concentration means to have a lower possibility to properly oxidate the carbonaceous particles.

The load strongly influences the concentration of particulate matter. In fact, when the load is increased (and so the air/fuel ratio decreases), PM emission increases a lot. This phenomenon can be seen on the following figure.

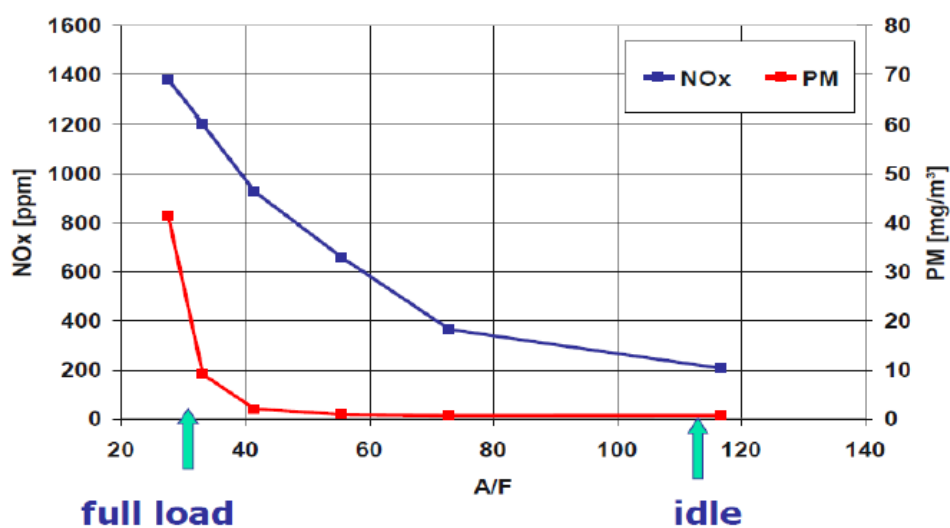


Figure 1.13 PM vs A/F ratio

It could be seen that until a certain A/F ratio, the load is not influencing a lot the emission. When a certain A/F ratio is reached, PM emissions have a steep increase. This value of A/F ratio is called “*smoke limit*” and normally is about 20 % more than the stoichiometric one.

Finally, increasing the injection advance is good for PM emission reduction.

Looking at the effect of EGR and injection advance on NO<sub>x</sub> and PM is possible see that they have the opposite behaviour. So, it is important to find a sort of “trade-off” between nitrogen oxides and particulate matter emission in order to keep both emission levels on an acceptable level.

## 1.4. Renewable fuel: HVO

The climate changing and the studies on the effect of using hydrocarbons on the human health, have pushed legislators to find a solution to those problems, considering also that conventional hydrocarbons are a non-renewable energy source.

Most recently, a new typology of biofuel was developed: the hydrotreated vegetable oil (HVO). The source of this fuel are vegetable oils and cooking oils. They are a mixture of paraffinic hydrocarbons that are sulphur free and without aromatics, giving it an higher cetane number with respect the conventional diesel [5].

In the following figure [6] the production process is shown: starting from triglycerides, hydrogen is added in order to break them into monoglycerides, diglycerides and carboxylic acids. These are the precursors of the iso-alkanes used from transportation: thanks to another hydrogenated process (with or without carbon removal) they are formed into n- and iso-alkanes.

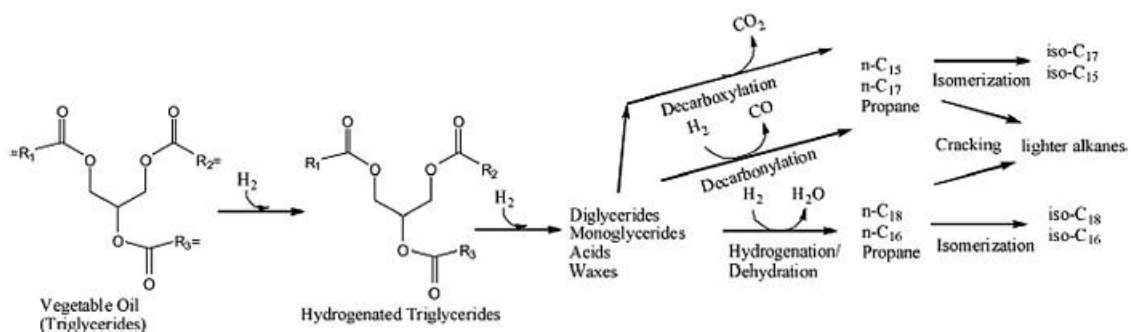


Figure 1.14 Production process of HVO

Although some studies analysed the effect of this fuel on emission, there is still lack of information about the impact into emission levels.

## 2. General information about the tool

This Matlab tool uses two different kind of combustion models: the first one is a one-zone model, while the second one is a three-zone model.

The first model is the simplest one and the hypothesis behind this model is that the mixture inside the cylinder is a thermodynamic system that exchange with the environment exchanging energy or mass. This allow us to obtain, for example, the heat release curve thanks to the first principle of the thermodynamics. Since the simplicity of the model, they do not allow to apply some submodel use for the evaluation of the emission of pollutant species.

The second one is a most complete model, where three different zones are identified inside the cylinder:

- Unburned gases zone
- Fuel zone
- Burned gases zone

Differently from the first model, it allows to be more precise since it is possible to apply different injection profile and different injection strategies. Moreover, it is possible to apply some submodel in order to estimate the trend of pollutant species (PM and NO<sub>x</sub>) crank angle by crank angle.

All this models are predictive models, so they use the pressure signal in order to evaluate the heat release rate, the fraction of the fuel mass that is burning or the evolution of the pollutant species inside the cylinder.

The compression ignition engine under test is a F1A engine, whose specification are shown in the following table:

<b>Engine type</b>	Euro 6d final diesel engine
<b>Number of cylinder</b>	4
<b>Valves for cylinder</b>	4
<b>Displacement</b>	2.3 L
<b>Bore</b>	88 mm
<b>Stroke</b>	94 mm
<b>Conrod length</b>	146 mm

<b>Compression ratio</b>	16.2
<b>Supercharging</b>	Single stage with eVGT
<b>IVO</b>	-36°
<b>IVC</b>	232°
<b>EVC</b>	9°
<b>EVO</b>	131°
<b>Wall temperature</b>	430 K
<b>Lower heating value Diesel</b>	42650 kJ/kg
<b>Lower heating value HVO</b>	44350 kJ/kg
<b>Diesel density</b>	830.6 kg/m <sup>3</sup>
<b>HVO density</b>	777.8 kg/m <sup>3</sup>

*Table 2.1 Engine and fuel specification*

This tool requires some input parameters in order to work properly, such as:

- The pressure signal in the combustion chamber of the cylinder number 1
- The pressure signal in the intake manifold of the cylinder number 1
- The electrical signal of the injector
- Data coming from the test bench

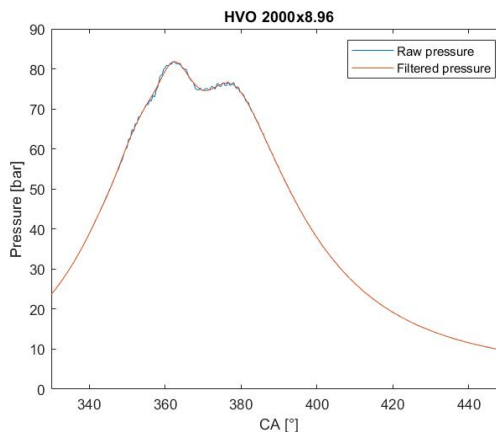
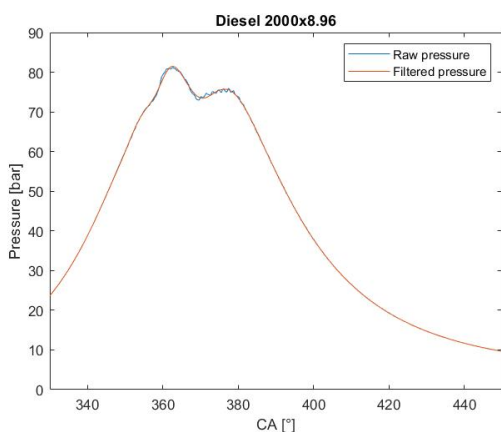
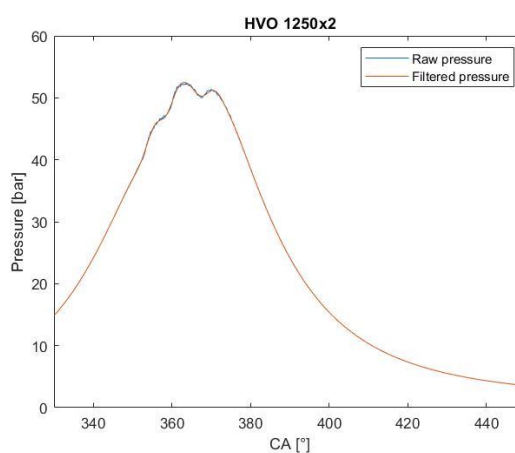
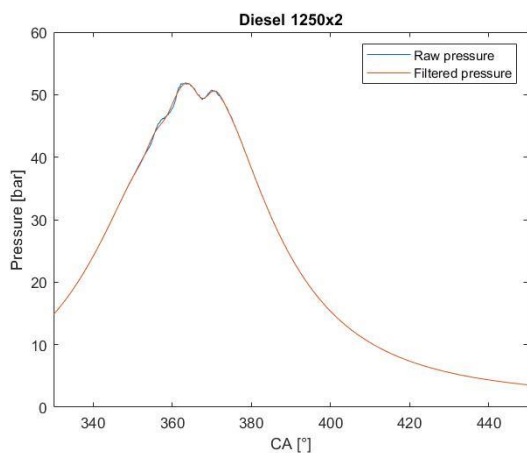
The first step to do is to properly measure and filter the pressure signal in order to have an accurate predictive model. The pressure is measured by some piezoresistive transducers, that convert the mechanical stress (such as compressive stress) into charge separation, that is subsequently converted into a voltage signal thanks to some amplifiers. This method has the drawback that is not able to measure an absolute pressure, so the pressure signal needs to be properly referenced. The method used inside the code is the TAF one, where the absolute pressure is obtained using the absolute pressure measured in the intake manifold by a transducer. The relation able the reference the in-cylinder pressure is the following:

$$p_{cyl,abs} = p_{cil} + (\bar{p}_{man} - \bar{p}_{cyl}) \quad Eq. 1$$

The mean cylinder pressure inside the brackets is measured in a crank angle interval of  $\pm 5^\circ$  crank angle degrees with respect the BDC ( $180^\circ$ ) with a step of  $0.1^\circ$ , while the mean intake manifold pressure is measured taking all  $720^\circ$  with a step of  $0.1^\circ$ .

Then, the pressure signal needs to be filtered since the signal is not so smooth due to the fact that the piezoresistive transducer is placed inside the glow-plug. The method used is the TAF one, that consist in approximate the pressure signal using a spline in an iterative way, until the error of approximation is greater than a certain value.

In the following diagrams the pressure trace before and after the filtering process is reported for all three working points and for both fuels:



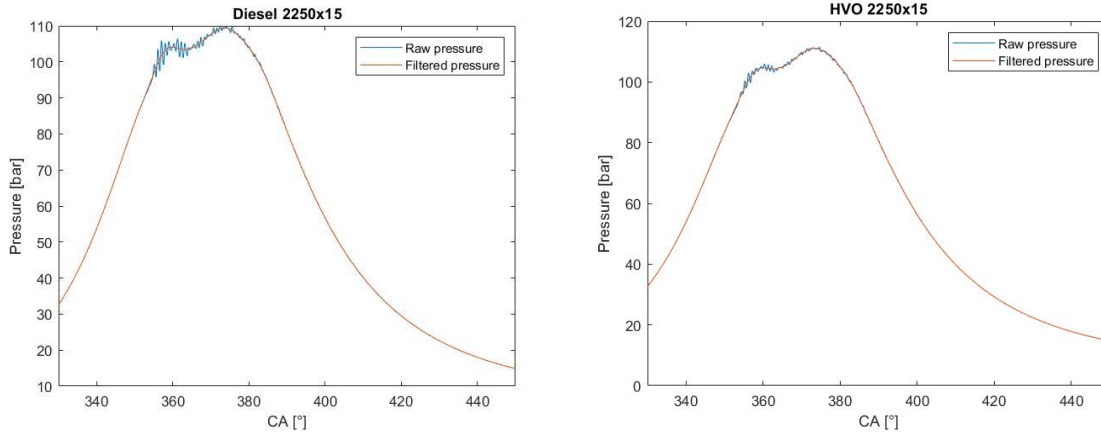


Figure 2.1 Pressure trend before and after the filtering process

From the above filter, it is possible to see that increasing the load and the engine speed the amplitude oscillation of the raw pressure increases.

Thanks to the geometrical parameters of the engine reported in the *Table 2.1*, it is possible to evaluate the instantaneous volume of the cylinder, that is useful in order to obtain the heat release curve.

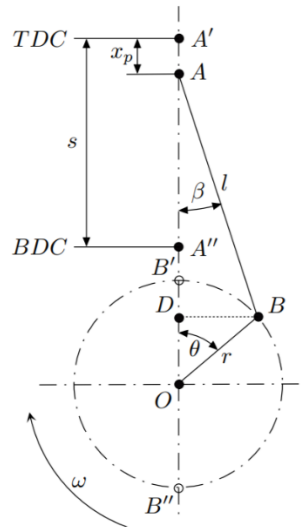


Figure 2.1 Principal geometric parameters for a crank mechanism [8]

From the above figure, using some simple geometric relations it is possible to write the instantaneous position of the piston with respect the bottom dead centre (BDC):

$$x = r \left[ (1 - \cos\theta) + \frac{1}{\Lambda} (1 - \cos\beta) \right] \quad \text{Eq. 2}$$

$\Theta$  is the angle that the crank forms with the cylinder axis,  $\beta$  is the inclination angle of the connecting rod and  $\Lambda$  is the so called “*elongation ratio*”, that is defined as the ratio between the crank radius and the connecting rod length:

$$\Lambda = \frac{r}{l} \quad \text{Eq. 3}$$

In order to have the instantaneous position of the position as function only of the angular position of the crank, it is applied the **sine theorem** to the two triangles ODB and ADB, in order to write  $\beta$  as function of  $\theta$ .

$$x = r \left[ (1 - \cos\theta) + \frac{1}{\lambda} \left( 1 - \sqrt{1 - \lambda^2 \sin^2\theta} \right) \right] \quad Eq. 4$$

Now it is possible to calculate the instantaneous value of the volume, that is the sum of a fixed part (the volume at TDC) and the part that depends on the piston position:

$$V = V_{dead} + \pi \frac{D^2}{4} \quad Eq. 5$$

$$V_{dead} = \frac{V_{disp}}{\varepsilon - 1} \quad Eq. 6$$

The trend of the instantaneous volume is reported below in the *Figure 2.2*

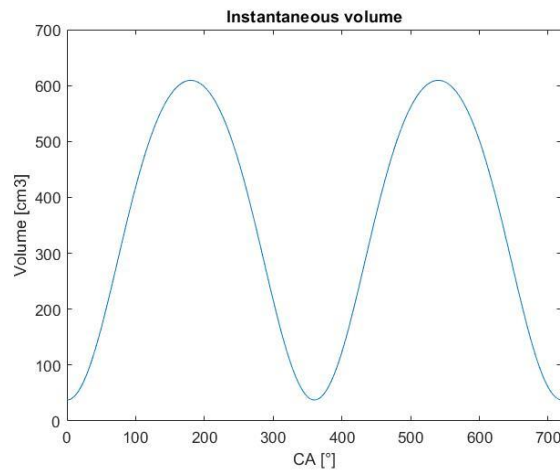


*Figure 2.2 Instantaneous volume trend*

### 3. One zone model

The one zone model is, as said before, the simplest of the two diagnostic models used in this work. The input data required in order to fully exploit the potential of this model are:

- Temperature in the intake manifold
- Temperature in the exhaust manifold
- Pressure in the intake manifold
- Pressure in the exhaust manifold
- Fuel mass flow rate
- EGR level
- Air mass quantity
- Global relative air/fuel ratio measured through the exhaust gases
- Absolute air humidity

The software used at the test bench gives as output different values of the EGR level, considering different ways to obtain this value (according to the CO<sub>2</sub> concentration in the intake manifold, to the intake manifold temperature and to the duct temperature). The value used for this work is the one evaluated according to CO<sub>2</sub> the concentration in the intake manifold according to the following formula:

$$X_r = \frac{[CO_2]_{int} - [CO_2]_{air}}{[CO_2]_{exh} - [CO_2]_{air}} \quad Eq. 7$$

#### 3.1. Trapped mass and mean temperature estimation

The trapped mass is evaluated using the global relative air/fuel ratio measured at the exhaust. Since in the one zone model is not the injection law, the hypothesis is that all the fuel is injected simultaneously and the trapped mass remains constant from the IVC to the EVO and is equal to:

$$m_{trap} = m_{air} + m_{res} + m_{EGR} + m_f \quad Eq. 8$$

- The mass of air is estimated using the air/fuel ratio, since the fuel quantity is known. Is it important to highlight that the UEGO sensor used to estimate the global relative air/fuel ratio considers only dry air, and not the wet one. So, a corrective factor has to be inserted in order to take into account the absolute humidity of the air.

$$m_{air} = \lambda_{exh} \alpha_{st} m_f (1 + H_{abs}) \quad Eq. 9$$

- The mass of residual gases (the gases of the previous engine cycle that remain inside the cylinder) is estimated considering the perfect gas law at the EVC:

$$m_{res} = \frac{p(EVC)V(EVC)}{RT_{exh}} \quad Eq. 10$$

- The mass of the recirculated exhaust gases is calculated using the definition of EGR rate:

$$X_r = \frac{m_{EGR}}{m_{EGR} + m_{air}} \quad Eq. 11$$

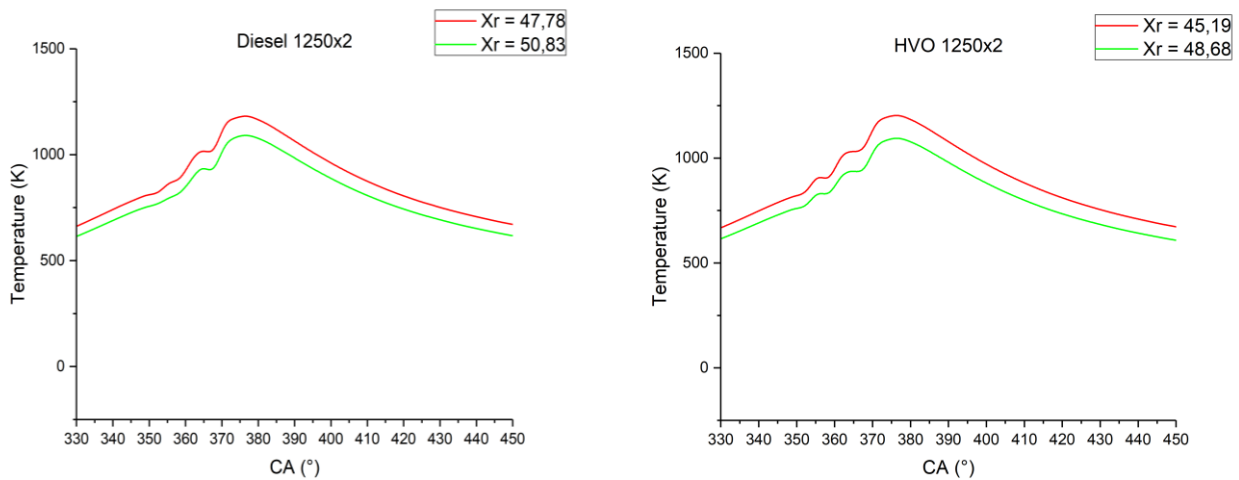
- The last mass that has to be evaluated is the fuel one. It is obtained from the fuel mass flow rate and the engine speed according the following formula:

$$m_f = \frac{\frac{\dot{m}_f}{3600N_{cyl}}}{\frac{n}{120}} \quad Eq. 12$$

Knowing the trapped mass value, is now possible to obtain the value of the mean temperature inside the cylinder, using the perfect gas law:

$$T_m = \frac{pV}{Rm_{trap}} \quad Eq. 13$$

The trend of temperature of some tests are reported below:



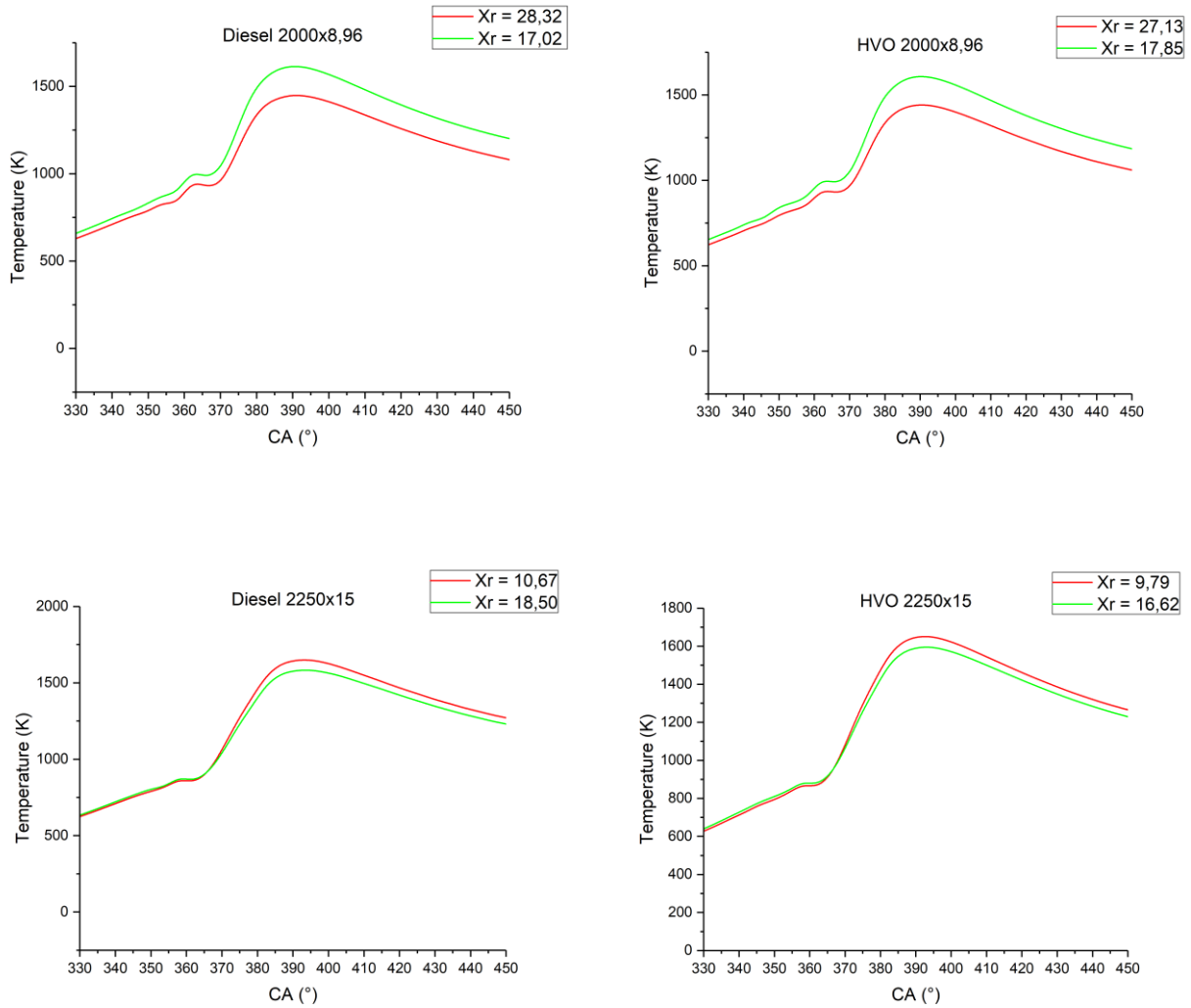


Figure 3.1 Mean temperature for all working point and both fuel with two different EGR levels

Looking at the above figure, it is possible to see that increasing the EGR rate the mean temperature increases since the mixture is more diluted.

### 3.2. SOC estimation and Heat Release Rate curve

In order to understand what is the point where the combustion process starts, it is used the motored pressure trace, that is the pressure inside the cylinder of a cycle without combustion. This pressure trace is constructed as sequence of two polytropic transformation, that go from IVC to the TDC and from TDC to the end of elaboration, that is 450°. To do this, the two exponents of the transformations have to be defined. Using the definition of the polytropic transformation, the two exponents are defined as follow:

$$m_{com} = \frac{\log\left(\frac{p_{SOI}}{p_{IVC}}\right)}{\log\left(\frac{V_{IVC}}{V_{SOI}}\right)} \quad Eq. 14$$

$$m_{exp} = \frac{\log\left(\frac{p_{EVO}}{p_{EOE}}\right)}{\log\left(\frac{V_{EOE}}{V_{EvO}}\right)} \quad Eq. 15$$

In the *Figure 3.2* are reported the motored pressure and the filtered one for a test conducted with diesel at 1250 rpm x 2 bar.

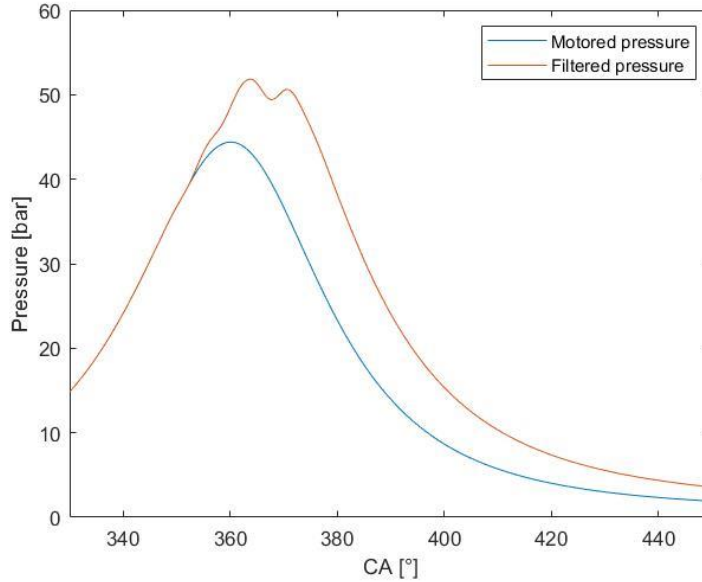


Figure 3.2 Motored pressure and filtered one for a diesel test (1250x2)

The SOC point is defined as the point where the two curves deviate of a certain quantity. In order to not overestimate the SOC, the threshold is fixed at 0.1%

However, it can happen that this method overestimate the value of the SOC. So a correction will be done looking at the curve of the net heat release rate (NHRR), defined as:

$$NHRR = \frac{\gamma}{\gamma - 1} p_i \frac{V_i - V_{i-1}}{\theta_i - \theta_{i-1}} + \frac{1}{\gamma - 1} V_i \frac{p_i - p_{i-1}}{\theta_i - \theta_{i-1}} \quad Eq. 16$$

The polytropic coefficient  $\gamma$  is a function of the temperature and the equation that correlates its value and the temperature was found by the previous thesis student through an interpolation [8]

$$\gamma = 1.392 - 8.13 * 10^{-5} T_m$$

It is known that the curve of the nHRR, after a long part of the compression stroke where it is negative, rises up and become positive. The SOC is so defined as the point where this curve starts to rises up. This correction is done going backward from the value of the SOC previously individuated to the SOI until the first minimum of the curve.

Integrating the curve of the nHRR is possible to obtain the  $Q_{net}$  trend.

For what regards the gross Heat Release Rate analysis, is fundamental to quantify the amount of heat exchanged between the charge and the cylinder walls. In order to do this, the Woschni model is used, that helps us to properly define the convective heat transfer coefficient.

The convective power exchanged with the wall is defined as follow:

$$\dot{Q}_{ht,conv} = h_{conv} [A_w (T_{gas} - T_w) + A_{head} (T_{gas} - T_w) + A_{piston} (T_{gas} - T_w)] \quad Eq. 18$$

The temperatures of piston and cylinder hear have been considered equal to the wall one. In this way the three surfaces could be condensed in only one:

$$A_{ht} = \pi D x + V_{min} \frac{\pi D}{\pi \frac{D^2}{4}} + 2 \left( \pi \frac{D^2}{4} \right) \quad Eq. 19$$

Through a big experimental campaign, Woschni was able to demonstrate that the convective heat transfer coefficient is function of the velocity of the mixture, of the pressure and temperature [9]. The expression is the following one:

$$h_{conv} = C_0 D^{-0.2} p^{0.8} T_m^{-0.53} w^{0.8} \quad Eq. 20$$

Where  $C_0$  is the calibration parameter.

The velocity of the mixture is given by the mean piston speed and by the expansion of the burned gases. It is defined as:

$$w = C_1 \bar{S}_p + C_2 \frac{V_d T_{ref}}{p_{ref} V_{ref}} (p - p_{motored}) \quad Eq. 21$$

The reference conditions are the one at the IVC, while  $C_1$  and  $C_2$  are constants depending on the engine stroke:

- $C_1 = (2.28 + 0.308 X_{swirl})$ ;
- $C_2 = 0.00324$

$X_{swirl}$  is the *swirl ratio* and in this case is equal to 0.1.

It is also considered the radiating heat power, defined as:

$$\dot{Q}_{ht,rad} = k_{rad} A_{ht} (T_{gas}^4 - T_w^4) \quad Eq. 22$$

Integrating the convective power and the radiative one the heat transferred to the wall is obtained and adding this value with  $Q_{net}$  is possible to obtain the gross heat released by the fuel ( $Q_{gross}$ ).

The calibration process consists in changing the value of  $C_0$  in order to obtain the following relation (since the combustion efficiency in this model is considered unitary):

$$Q_{gross}(EOC) = m_f LHV \quad Eq. 23$$

The acceptable values for the  $C_0$  coefficient is in a band between 50 and 300. So, it is important to consider what to do when the value arrives on the limit (upper or lower) and the model is not yet calibrated. There are two cases:

- If the value of the calibrating coefficient must be lower than 50, it means that the quantity of the fuel is underestimated, and so it is increased with a step of 0.01 mg until the model is calibrated;
- If the value of the calibrating coefficient must be greater than 300, it means that the quantity of the fuel is overestimated, and so it is decreased with a step of 0.01 mg until the model is calibrated

### 3.3. End of combustion (EOC)

The end of combustion is a point that is tricky to find. One of the ways used to define it is to assume a certain threshold of the HRR under which the combustion could be considered finished. The threshold used is fixed at 2% of the peak of the HRR. Since the EOC is function of the HRR, it means that also the EOC point is a function of the calibrating coefficient  $C_0$ . In the previous work was proved that, considering only the threshold method, a certain quantity of energy will be discard. In order to avoid this phenomenon, an arbitrary quantity of  $25^\circ$  was added to the threshold value [10].

### 3.4. Mass fraction burned and combustion metrics

The mass fraction burned is the percentual expression of the net heat release, in order to easily compare different tests. The instantaneous value of the mass fraction burned is defined as:

$$x_b = \frac{Q_{net}}{Q_{net}(EOC)} \quad Eq. 24$$

This parameter is useful in order to define the some combustion metrics, such as MFB5, MFB10, MFB50 (very important because it is considered such a “barycentre” of the combustion process) and MFB90 (that gives us the idea of when the combustion in the final part).

### 3.5. Tables and graphical results

Pressure File	Engine Point	EGR rate [%]	EOC [°]	$C_0$
------------------	-----------------	-----------------	------------	-------

32	1250x2	47.78	421.4	80
33	1250x2	50.83	422.1	89
34	1250x2	49.99	421.6	94
35	1250x2	48.11	421.2	87
36	1250x2	47.79	421	76
37	1250x2	47.91	421.2	87
38	1250x2	47.82	420.9	80
3	2000x8.96	28.32	451.3	117
4	2000x8.96	26.96	451	115
5	2000x8.96	25.76	450.5	112
6	2000x8.96	23.99	450.6	113
7	2000x8.96	21.84	451.1	113
8	2000x8.96	19.21	450.2	114
9	2000x8.96	17.02	450.9	117
3	2250x15	19.52	460	134
4	2250x15	10.67	459.2	134
5	2250x15	12.49	458.4	136
6	2250x15	13.30	457.6	135
7	2250x15	15.21	456.1	134
8	2250x15	16.07	456.7	133
9	2250x15	16.73	460.1	129
10	2250x15	18.50	459.3	133

*Table 3.1 Calibration data for test conducted with diesel*

Pressure File	Engine Point	EGR rate [%]	EOC [°]	C0
32	1250x2	45.19	420.4	109
33	1250x2	48.68	420.4	118

34	1250x2	47.52	419.7	109
35	1250x2	45.50	420.9	116
36	1250x2	45.04	420.7	110
37	1250x2	45.19	421	111
38	1250x2	45.16	420.8	112
3	2000x8.96	27.13	449	126
4	2000x8.96	26.21	448.7	125
5	2000x8.96	25.56	449.8	127
6	2000x8.96	24.16	450.9	128
7	2000x8.96	22.72	448.4	130
8	2000x8.96	20.86	448.6	128
9	2000x8.96	17.85	451.2	129
3	2250x15	18.32	461.2	166
4	2250x15	9.79	461.9	165
5	2250x15	11.20	461.8	165
6	2250x15	12.09	460	165
7	2250x15	13.83	462.1	162
8	2250x15	14.28	460.3	162
9	2250x15	15.21	462.1	164
10	2250x15	16.62	460.7	163

*Table 3.2 Calibration data for tests conducted with HVO*

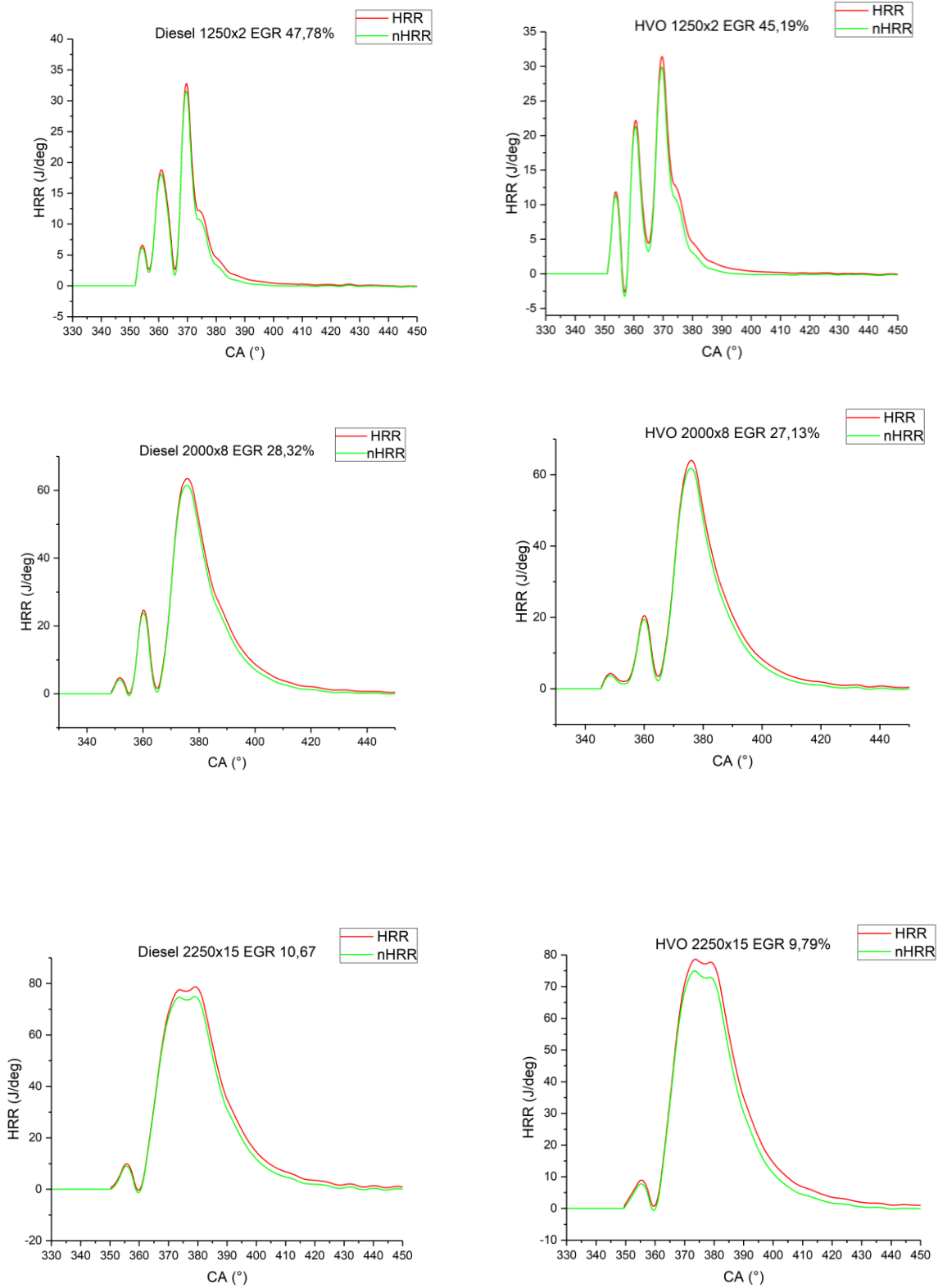
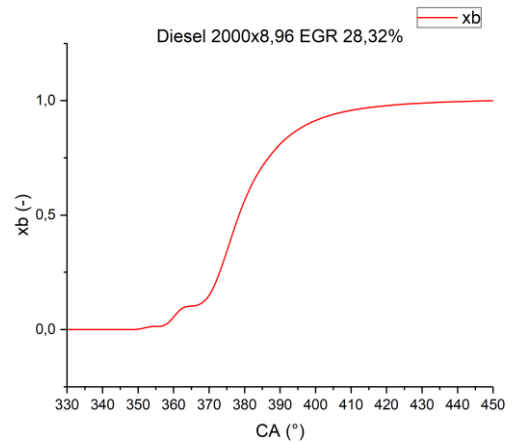
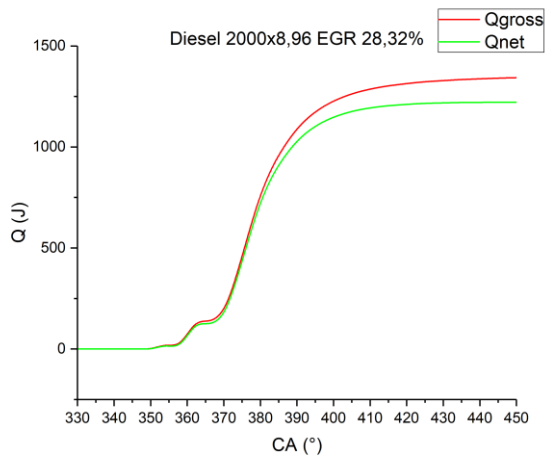
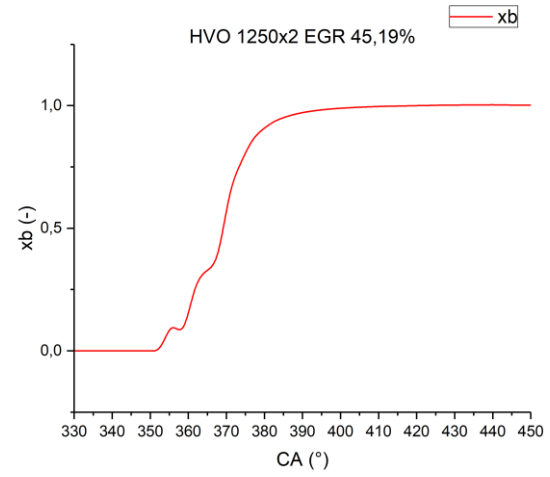
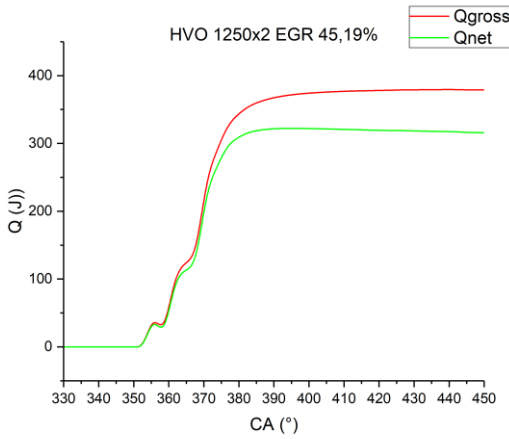
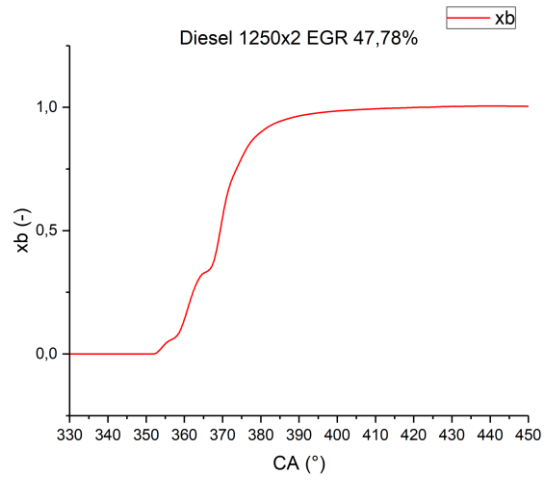
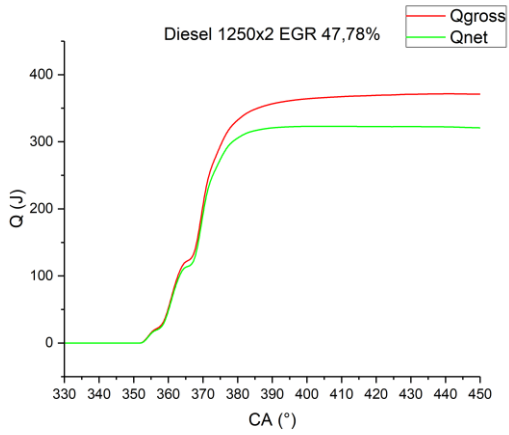


Figure 3.3 Heat release rate (gross and net) curve for all working point and for both fuels



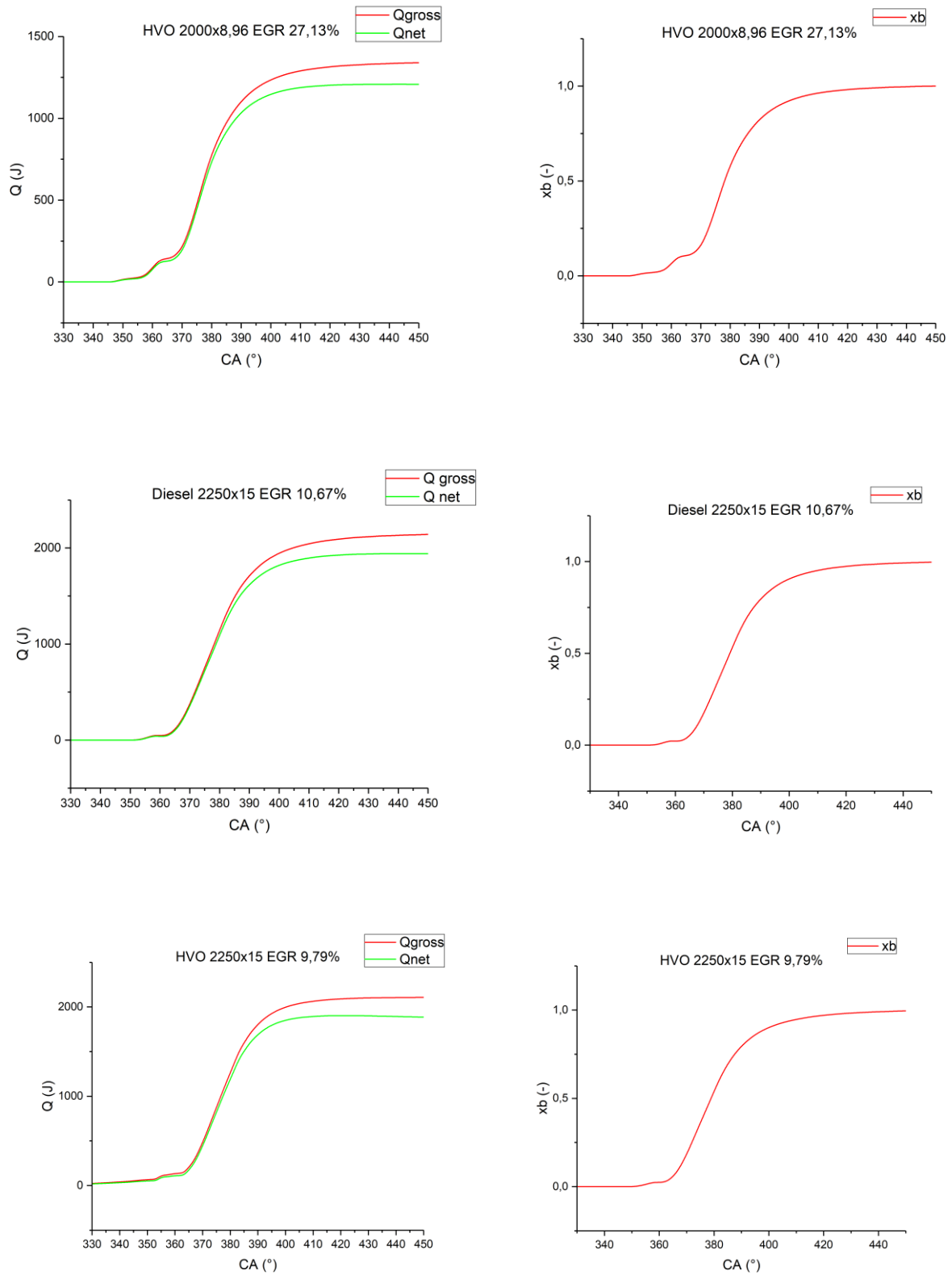


Figure 3.4 Gross and net curves (on the left) and mass fraction burned curves (on the right)

Pressure	Engine	EGR rate	MFB5	MFB10	MFB50	MFB90
----------	--------	----------	------	-------	-------	-------

File	Point	[%]				
32	1250x2	47.78	-4.43	-1.05	9.28	19.98
33	1250x2	50.83	-2.35	-0.41	9.70	20.37
34	1250x2	49.99	-2.51	-0.51	9.55	20.37
35	1250x2	48.11	-3.66	-0.93	9.32	19.98
36	1250x2	47.79	-4.23	-1.09	9.24	19.83
37	1250x2	47.91	-4.36	-0.98	9.29	19.96
38	1250x2	47.82	-4.34	-1.03	9.25	19.84
3	2000x8.96	28.32	-0.34	3.56	18.33	38.04
4	2000x8.96	26.96	-0.44	3.16	18.17	37.55
5	2000x8.96	25.76	-0.41	3.86	18.17	37.56
6	2000x8.96	23.99	-0.60	3.12	18.02	37.09
7	2000x8.96	21.84	-0.58	3.88	17.98	37.00
8	2000x8.96	19.21	-0.76	3.77	17.87	36.68
9	2000x8.96	17.02	-0.88	3.52	17.76	36.43
3	2250x15	19.52	4.93	7.59	19.73	41.30
4	2250x15	10.67	4.69	7.26	19.03	39.12
5	2250x15	12.49	4.75	7.34	19.21	39.81
6	2250x15	13.30	4.77	7.36	19.22	39.92
7	2250x15	15.21	4.81	7.41	19.34	40.36
8	2250x15	16.07	4.80	7.42	19.41	40.48
9	2250x15	16.73	4.85	7.49	19.49	40.54
10	2250x15	18.50	4.85	7.49	19.53	40.71

*Table 3.3 Combustion metrics for tests conducted with diesel*

Pressure File	Engine Point	EGR rate [%]	MFB5	MFB10	MFB50	MFB90
32	1250x2	45.19	-6.27	-1.33	9.07	19.25

33	1250x2	48.68	-5.92	-0.99	9.41	19.60
34	1250x2	47.52	-6.10	-1.25	9.20	19.14
35	1250x2	45.50	-6.16	-1.17	9.17	19.50
36	1250x2	45.04	-6.29	-1.40	9.06	19.21
37	1250x2	45.19	-6.28	-1.34	9.08	19.32
38	1250x2	45.16	-6.27	-1.33	9.06	19.36
3	2000x8.96	27.13	-1.08	2.91	18.01	36.81
4	2000x8.96	26.21	-1.14	2.72	17.90	36.65
5	2000x8.96	25.56	-1.16	2.69	17.88	36.75
6	2000x8.96	24.16	-1.24	2.70	17.77	36.42
7	2000x8.96	22.72	-1.33	2.64	17.77	36.53
8	2000x8.96	20.86	-1.39	2.66	17.67	36.32
9	2000x8.96	17.85	-1.46	2.57	17.55	35.82
3	2250x15	18.32	4.50	7.23	19.38	41.68
4	2250x15	9.79	4.30	6.96	18.81	39.78
5	2250x15	11.20	4.39	7.05	19.00	40.39
6	2250x15	12.09	4.40	7.07	18.98	40.05
7	2250x15	13.83	4.45	7.12	19.13	40.82
8	2250x15	14.28	4.44	7.12	19.08	40.28
9	2250x15	15.21	4.43	7.15	19.20	40.92
10	2250x15	16.62	4.44	7.17	19.21	40.72

*Table 3.4 Combustion metrics for tests conducted with HVO*

## 4. Three zone model

The three zone model is a simplification of the Dec's combustion model [4], since the evaporative submodel is not implemented in this tool and the premised phase is not considered. The combustion chamber is subdivided into three different zones:

- A zone where there is present only fuel (*fuel zone*)
- A zone of only burned gases, obtained considering a global stoichiometric combustion (*burned zone*)
- A zone of only unburned gases (*unburned zone*). In other words in this zone there are air, residual gases and recirculated exhaust gases

The trapped quantity of unburned gases is calculated in the same way done for the one zone model, with the only change that now the injection profile is simulated and so the profile of the trapped mass changes according to the fuel injections.

An important hypothesis that is done is that the three zones are considered homogeneous and the gases are considered ideal, so the pressure is the same in all the three zones.

This diagnostic model is subdivided mainly in three angular intervals, where a different number of zones are present:

- Between the IVC and the SOI, inside the cylinder there is only the air that comes from the intake manifold (fresh air + EGR) and the residual gases of the previous cycle. So, it is possible to use a one zone approach since the only zone that is present is the unburned one;
- Between SOI and SOC there is the introduction of the fuel. In this case a two zone approach is used since now there is also the "fuel zone";
- Between SOC and EOC the reactants contained in the fuel zone and in the unburned one react each other in a stoichiometric way in order to generate the third zone, that is the burned one.

The model is based on the resolution of a closed system of thermodynamics equations applied to each zone. The equations present in this closed system are energy conservation equations and mass conservation one.

$$\delta Q_u + V_u dp = d(m_u i_u) + dm_{u \rightarrow b} i_u \quad \text{Eq. 25}$$

$$\delta Q_f + V_f dp = d(m_f i_f) - dm_{f,inj} i_{f,inj} + dm_{f \rightarrow b} i_f \quad \text{Eq. 26}$$

$$\delta Q_b + V_b dp = d(m_b i_b) - dm_{u \rightarrow b} i_u - dm_{f \rightarrow b} i_f \quad \text{Eq. 27}$$

The first term of the first member represents the heat transfer between the zone and the cylinder walls; the first term of the second member represents the internal

enthalpy of each zone and the second term of the second member is the incoming or outgoing enthalpy (when the sign is positive, enthalpy is coming out).

Now are presented also the mass conservation equations:

$$dm_u = -dm_{u \rightarrow b} \quad \text{Eq. 28}$$

$$dm_f = dm_{f, inj} - dm_{f \rightarrow b} \quad \text{Eq. 29}$$

$$dm_b = dm_{u \rightarrow b} + dm_{f \rightarrow b} \quad \text{Eq. 30}$$

Another important equation that is important for the model is the definition of the unburned stoichiometric value, since the hypothesis of stoichiometric combustion:

$$\frac{dm_{u \rightarrow b}}{dm_{f \rightarrow b}} = \alpha_{st}^u \quad \text{Eq. 31}$$

The unburned stoichiometric value is different from the fresh air one, since takes into account that there are also EGR e residual gases. The expression of the unburned stoichiometric value is the following:

$$\alpha_{st}^u = \left( \frac{m_u}{m_f} \right)_{st} = \left( \frac{m_{air} + m_{EGR} + m_{res}}{m_f} \right)_{st} \quad \text{Eq. 32}$$

This value depends of the content of oxygen in the unburned zone, that in turn depends on the concentration of residual and EGR gases inside the cylinder. In literature was demonstrated that there is a dependence between the oxygen concentration (and so the unburned stoichiometric ratio) and a parameter  $X_r/\lambda$ , where  $X_r$  is the total fraction of the residual gases and it is described by the following relation:

$$X_{r, tot} = \frac{m_{EGR} + m_{res}}{m_{EGR} + m_{res} + m_{air} + m_{f, inj}} \quad \text{Eq. 33}$$

The trend of the unburned stoichiometric ratio as function of the above mentioned parameter is reported in the *Figure 4.1* [11].

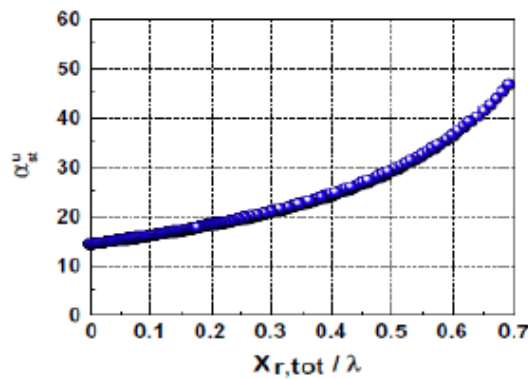


Figure 4.1 Trend of the unburned stoichiometric ratio as function of the parameter  $X_r/\lambda$

Increasing the total fraction of the residual gases maintaining constant the value of the  $\lambda$  causes an increasing of the unburned stoichiometric ratio because the quantity of recirculated gases increases and the oxygen concentration decreases. Decreasing  $\lambda$  maintaining constant  $X_{r,tot}$  causes an increasing of the unburned stoichiometric ratio

because the oxygen concentration in the exhaust gases decreases (decreasing  $\lambda$  means increasing the load) and so the oxygen concentration in the intake manifold decreases.

The following relation that bonds the unburned stoichiometric ratio and the parameter  $X_{r,tot}/\lambda$  is obtained from the above graph thanks to a polynomial interpolation of the fourth order:

$$\alpha_{st}^u = 132.08 \left( \frac{X_{r,tot}}{\lambda} \right)^4 - 78.471 \left( \frac{X_{r,tot}}{\lambda} \right)^3 + 38.115 \left( \frac{X_{r,tot}}{\lambda} \right)^2 + 13.695 \frac{X_{r,tot}}{\lambda} + 14.379 \quad Eq.34$$

In [11] are also treated the specific enthalpies of the different zones and it is demonstrated that using a second order polynomial correlation is sufficient to properly describe the variation of temperature and mass inside the zones. The enthalpy of the fuel zone is assumed to be only function of the temperature. For what regard the specific enthalpy of the burned gases, a stoichiometric combustion is considered and the products of the reaction are  $CO_2$ ,  $H_2O$ ,  $O_2$ ,  $N_2$ ,  $O$ ,  $OH$ ,  $H$  and  $NO$ . The enthalpy of this zone is calculated through a weighted mean between all these products and the enthalpy value of each species (dependent on temperature) is taken from the JANAF tables. Finally, the specific enthalpy is calculated through a weighted mean between the air enthalpy and the exhaust gases one, in order to take into account the residual gases and the EGR ones.

All these enthalpies are function of different parameters, such as the chemical composition (and so the parameter used previously to obtain the trend of the unburned stoichiometric ratio), the temperature and pressure (that influence, for example, the dissociation process). But it has been demonstrated that the parameter that mainly influence the enthalpy is the temperature. So, the enthalpies are described according to a second order polynomial equation dependent on the temperature:

$$i_j = a_j T_j^2 + b_j T_j + c_j \quad Eq.35$$

The heat transfer to the wall of each zone is simulated using the Woschni correlation for what regards the convective portion, as done in the one zone model. The remaining portion of the heat transfer is the radiative heat transfer, that now is important because of the presence of the soot.

$$Q_j = h_{conv,j} A_j (T_j - T_w) + k_{rad} A_j (T_j^4 - T_w^4) \quad Eq.36$$

The heat transfer to the wall is evaluated only for the burned and unburned regions, since the temperature of the fuel zone is close to the wall one. The temperature of the fuel at the exit of the injector is assumed to be dependent on the  $bmep$ , according to the following formula:

$$T_{fuel} = 413 + \frac{60}{19} (bmep - 1) \quad Eq.37$$

The expression for the convective heat transfer coefficient remains the same used in the one zone model (Eq.20), but there is only a small difference in the evaluation of the velocity of the charge: in fact, before the SOC the velocity of the charge is defined only by the mean piston speed, since there are not yet burned gas that are expanding.

In the expression of the heat transfer to the wall, the exchange surface are evaluated in a different way, considering what zone we are dealing of. The surface of each zone is obtained as a weighted average of the total surface (the one used for the one zone model).

In order to solve the closed system of equations, the conservation of mass laws have been integrated in order to have the mass of the fuel zone and the unburned one as function of the mass of the burned zone:

$$m_f = m_{f,inj} - \frac{m_b}{1 + \alpha_{st}^u} \quad Eq. 38$$

$$m_u = m_{trap} - \frac{m_b}{1 + \alpha_{st}^u} \alpha_{st}^u \quad Eq. 39$$

Considering that the volume displaced by the piston crank angle by crank angle is equal to the sum of volumes of the three zones and using the perfect gas law, the following relation could be written:

$$m_b = \frac{pV - m_{trap}R_uT_u - m_{f,inj}R_fT_f}{R_bT_b - \frac{\alpha_{st}^u}{1 + \alpha_{st}^u}R_uT_u - \frac{1}{1 + \alpha_{st}^u}R_fT_f} \quad Eq. 40$$

Now it is possible to rewrite the energy conservation equations in a form that allows us to discretize them.

$$\delta Q_u + V_u dp = m_u di_u \quad Eq. 41$$

$$\delta Q_f + V_f dp = m_f di_f + dm_{f,inj} (i_f - i_{f,inj}) \quad Eq. 42$$

$$\delta Q_b + V_b dp = m_b di_b + \frac{dm_b}{1 + \alpha_{st}^u} \alpha_{st}^u (i_b - i_u) + \frac{dm_b}{(1 + \alpha_{st}^u)} (i_b - i_f) \quad Eq. 43$$

Using the acquisition step of  $0.1^\circ$ , it is possible to approximate the differential to the difference of the finite values, since the step is very little.

One of the last information needed to start the elaboration of the three zone model is to know the temperature of the burned zone at the SOC point. This relation is obtained in [11] assuming that at that point the enthalpy of the reactants is equal to the products one.

$$T_b^{SOC} = -6.8 * 10^{-11} (i_u^{SOC})^2 + 5.3 * 10^{-4} i_u^{SOC} + 2434.349 \quad Eq. 44$$

For what regard the zone temperatures evaluation, there is a polynomial correlation of the second order that links the temperature with some experimental coefficients [11]:

$$a_j^{II} (T_j^i)^2 + b_j^{II} T_j^i + c_j^{II} = 0 \quad Eq. 45$$

In the following two tables are reported the coefficients of the polynomial correlation for both enthalpies and temperature [11].

	$a_j$	$b_j$	$c_j$
<b>f</b>	1.44590	860.78	- 949736
<b>u</b>	0.09983	982.30	- 477140 + - 2817105 $\frac{X_{r,tot}}{\lambda}$
<b>b</b>	0.31703	$\left( \begin{array}{l} 426.31+ \\ -0.68863p \end{array} \right)$	-2851737 + 517.97p + +2.3173 p <sup>2</sup>

Table 4.1 Coefficients for the estimation of the enthalpies

	$a_j^H$	$b_j^H$	$c_j^H$
<b>f</b>	$(m_f^i + \Delta m_{f,inj}) a_f$	$\left[ (m_f^i + \Delta m_{f,inj}) b_f - \frac{m_f^i R_f \Delta p}{p^i} \right]$	$-\dot{Q}_f^{i-1} \Delta t + (m_f^i + \Delta m_{f,inj}) c_f - m_f^i i_f^{i-1} +$ $-\Delta m_{f,inj} i_{f,inj}^i$
<b>u</b>	$m_u^i a_u$	$\left[ m_u^i b_u - \frac{m_u^i R_u \Delta p}{p^i} \right]$	$-\dot{Q}_u^{i-1} \Delta t + m_u^i [c_u - i_u^{i-1}]$
<b>b</b>	$[m_b^i + \Delta m_b] a_b$	$[m_b^i + \Delta m_b] b_b - \frac{m_b^i R_b \Delta p}{p^i}$	$-\dot{Q}_b^{i-1} \Delta t + [m_b^i + \Delta m_b] c_b +$ $-m_b^i i_b^{i-1} - \frac{\Delta m_b}{1 + \alpha_{st}^u} \alpha_{st}^u i_u^i - \frac{\Delta m_b}{1 + \alpha_{st}^u} i_f^i$

Table 4.2 Coefficients for the estimation of the temperatures

In the last table there are present the elasticity constants for the three zones and these values are considered constant:

- $R_u = 289$  J/kgK
- $R_b = 289$  J/kgK
- $R_f = 56.176$  J/kgK

For what regard the SOC individuation, at the beginning it is used an algorithm similar to the one used for the one zone model, with the difference that in the one zone model a relative threshold was established between the motored pressure and the filtered one, while in this case it is used an absolute difference equal to 0.001.

Regarding the EOC individuation, the threshold of the 2% of the peak value of the HRR curve is maintained as the one used in the one zone model, but in this case the

experimental campaign conducted by the previous thesis student suggests to add an angle of  $40^\circ$  to the angle obtained with the threshold method [8].

## 4.1. Injection profile

Dealing with three zone models, it is clear that it is important knowing how much fuel is injected crank angle by crank angle. In order to know this quantity it is important to construct a proper injection profile. Real life injection profiles have complex shape that are difficult to simulate. For this reason it is used a simplified model of the injection profile, assuming that it has a triangular shape. In the following figure it is reported the current profile and the injection one [8].

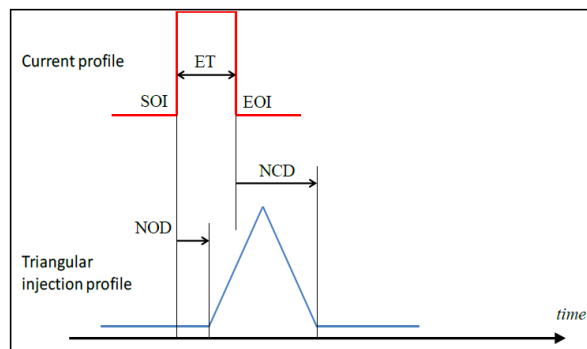


Figure 4.2 Current and injection profile

It is possible to analyse the quantity that are present in the above figure:

- SOI is the instant in which the electrical signal arrives to the injector connector in order to excite the solenoid. This point is taken analysing the current trace of the current clamp, and is the point in which the current overruns a certain threshold.
- NOD is the so called “*Nozzle opening delay*” and is the interval between the electrical SOI and the hydraulic one (when the real fuel injection starts)
- NCD is the so called “*Nozzle closing delay*” and is the interval between the electrical end of injection and the hydraulic one (the needle requires some time to reach its seat)
- ET is the “*Energizing time*” and it describes the duration of the electrical signal.

NOD and NCD are estimated practising a huge experimental campaign, and their values are defined as function of the rail pressure or as function of the ET.

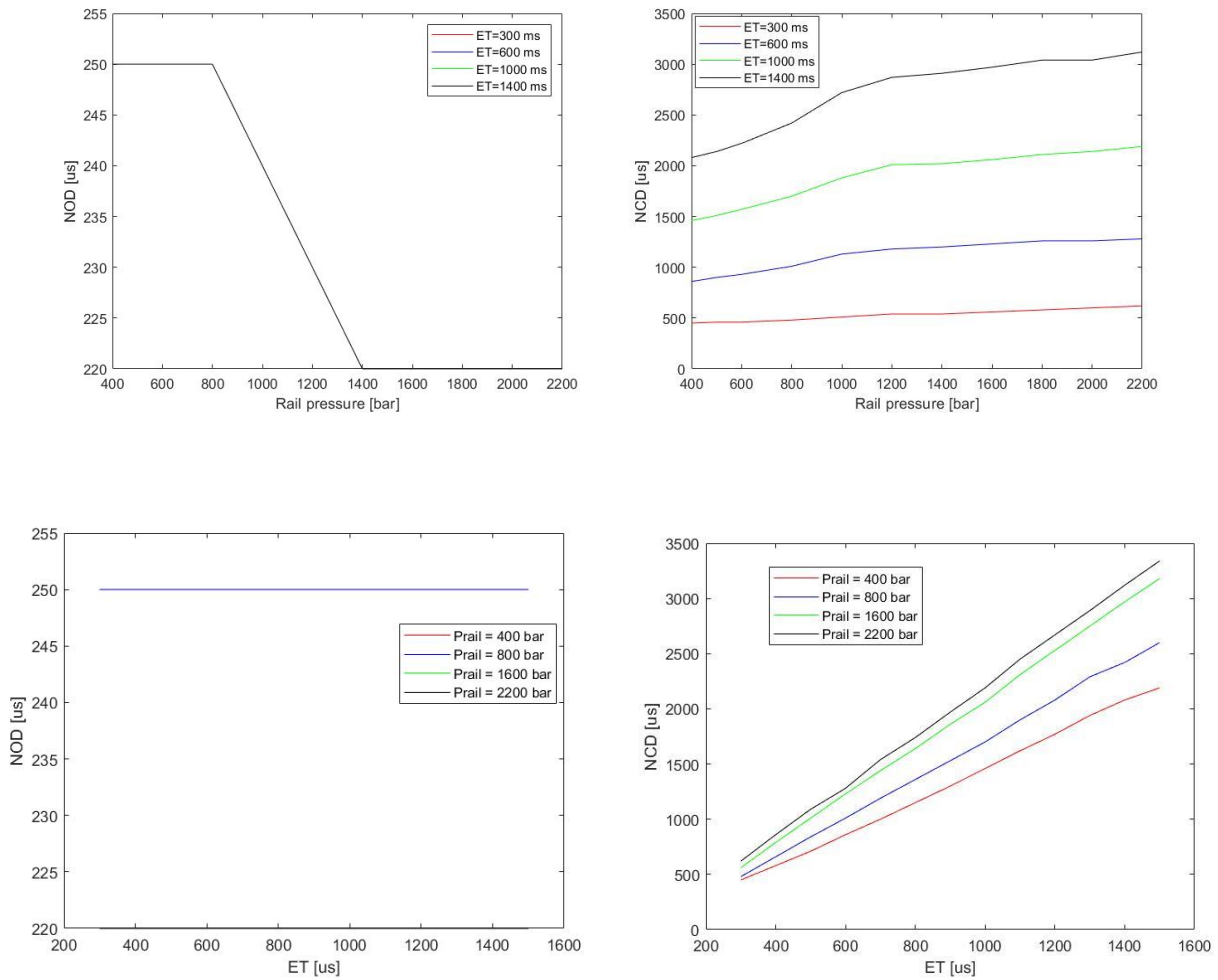


Figure 4.3 NOD and NCD as functions of ET and  $p_{rail}$

From the above figure it is possible to see that the NOD is less dependent on the parameters analysed with respect to the NCD. NOD slightly decreases when the rail pressure increases, while it is practically independent on the ET. NCD has an increasing trend both increasing the ET or the rail pressure. In the model could happen that some pilot injection has an ET that is lower than the lower limit of the back-up table. In this case, NOD and NCD are defined without interpolating and their values are:

$$NOD = 220 \mu s$$

$$NCD = 450 \mu s$$

From the excel data (coming from the test bench) the quantity of the fuel injected for each injection event is known, so it is possible to sketch the fuel mass flow rate as function of the ITL (*Injection timing length*), defined as:

$$ITL = ET + NCD - NOD \tag{Eq. 46}$$

Since the injection profile is assumed symmetric (the descending part is specular to the increasing one), it is possible to write the instantaneous fuel flow rate as function of the maximum flow rate. The relation of the increasing part of the injection is reported below:

$$\dot{m}_{f,inj} = \frac{2\dot{m}_{f,inj,max}}{ITL} \theta \quad Eq. 47$$

Where the maximum fuel flow rate is calculated knowing how many fuel is injected in this injection event

$$\dot{m}_{f,inj,max} = \frac{2m_{f,inj,tot}}{ITL} \quad Eq. 48$$

An example of injection profile and injected mass is reported below:

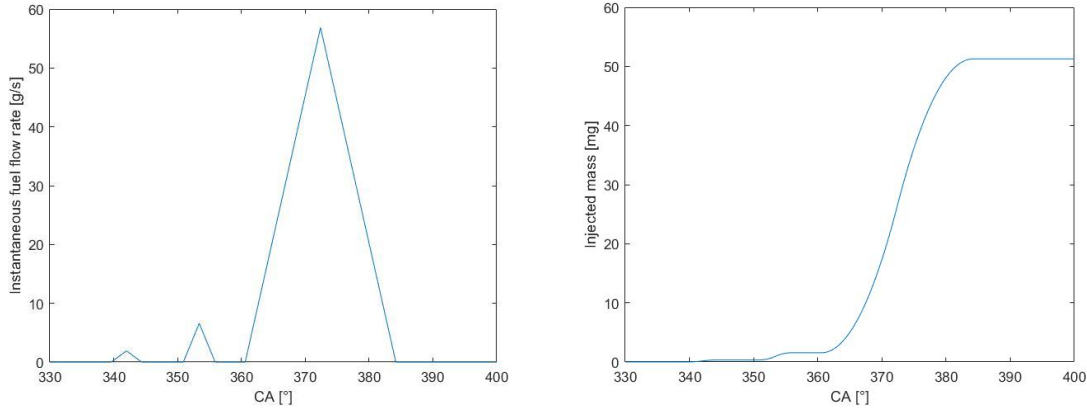


Figure 4.4 Example of injection profile and injected mass (Diesel 2250x15)

## 4.2. Model calibration

The three zone model is calibrated under three aspects: SOC identification, heat transfer coefficient calibration and calibration of the pilot injection.

For what regards the SOC identification, the procedure above mentioned could lead to an underestimation of the real SOC. In order to avoid this problem, a check is inserted inside the code: if the burned region mass is lower than 0, this means that the combustion has not yet started, and so the SOC is shifted by  $0.1^\circ$ .

The calibration of the Woschni heat transfer model requires to determinate the parameter  $C_0$ , but the process used to determinate it is quite different from the one used in the one zone model. In fact, in the three zone model the combustion efficiency is not unitary, since some pollutant species are measured at the exhaust. The concentration of these species is used to calculate the experimental combustion efficiency of the engine, that is defined as:

$$eff_{exp} = 1 - \frac{\dot{m}_{HC}LHV_{HC} + \dot{m}_{CO}LHV_{CO} + \dot{m}_{soot}LHV_{soot}}{\dot{m}_{fuel,tot}LHV} \quad Eq. 49$$

Where the lower heating values of the pollutant species are:

$$\text{LHV}_{\text{HC}}=42700 \text{ kJ/kg}$$

$$\text{LHV}_{\text{CO}}=10500 \text{ kJ/kg}$$

$$\text{LHV}_{\text{soot}}=38000 \text{ kJ/kg}$$

On the other hand, the calculated efficiency is the value of the mass fraction burned at the EOC, that whose trend is obtained from the mass of the burned gases

$$x_b = \frac{m_b}{(1 + \alpha_{st}^u)m_{fuel,tot}} \quad \text{Eq. 50}$$

The calibration of the parameter  $C_0$  continues until the absolute difference between the two efficiencies is lower than 0.0005. As seen in the one zone model, the acceptable value for this parameter are between 50 and 300. When it tends to become lower than 50, it means that the fuel quantity is underestimated and a quantity of 0.01 mg (this quantity in the next tables will be called  $mq$ ) is added to the main injection until the model is calibrated. On the contrary, if the parameter value tends to be greater than 300, it means that the fuel quantity is overestimated and a quantity of 0.01 mg is removed from the main injection until the model is calibrated.

The last calibration is done at the pilot injection level. In fact, could happen that the quantity injected during the first pilot injection is lower than the one that burns according to the pressure signal and the fuel zone mass assumes negative values. This is not physical and the problem is solved adding a step quantity of 0.1 mg (this quantity will be called  $pq$ ) until this problem is solved.

The results of the calibration process are showed below:

Pressure File	Engine Point	EGR rate [%]	SOC [°]	EOC [°]	C0	pq [mg]	mq [mg]
32	1250x2	47.78	353.3	388.7	50	0.6	0.32
33	1250x2	50.83	353.5	389.2	50	0.6	0.5
34	1250x2	49.99	353.5	388.9	50	0.6	0.4
35	1250x2	48.11	353.4	389.2	50	0.6	0.38
36	1250x2	47.79	353.4	389.4	50	0.7	0.45
37	1250x2	47.91	353.3	388.9	50	0.6	0.33
38	1250x2	47.82	353.4	389.2	50	0.7	0.39
4	2000x8.96	26.96	349.3	416.2	50	0.6	0.22
5	2000x8.96	25.76	349.2	416.2	50	0.6	0.27
6	2000x8.96	23.99	348.9	415.9	50	0.7	0.25

7	2000x8.96	21.84	348.7	415.8	50	0.6	0.26
8	2000x8.96	19.21	347.8	414.5	50	0.6	0.26
9	2000x8.96	17.02	346.9	413.4	50	0.6	0.2
3	2250x15	19.52	352.7	425.8	50	0	0.27
4	2250x15	10.67	351.5	422.8	50	0	0.78
5	2250x15	12.49	352.2	422.3	50	0	0.6
6	2250x15	13.30	352.2	422.3	50	0	0.6
7	2250x15	15.21	352.5	422.1	50	0	0.43
8	2250x15	16.07	352.6	426.7	50	0	0.46
9	2250x15	16.73	352.7	425.9	50	0	0.6
10	2250x15	18.50	352.8	425.3	50	0	0.37

Table 4.1 Calibration results for tests conducted with diesel

Pressure File	Engine Point	EGR rate [%]	SOC [°]	EOC [°]	C0	pq [mg]	mq [mg]
32	1250x2	45.19	352	386.5	50	0.8	0.59
33	1250x2	48.68	352.4	386.1	50	0.7	0.66
34	1250x2	47.52	352.4	386	50	0.7	0.68
35	1250x2	45.50	352.2	386	50	0.7	0.54
36	1250x2	45.04	351.9	386.1	50	0.7	0.58
37	1250x2	45.19	352	386.1	50	0.7	0.56
38	1250x2	45.16	352	386.1	50	0.8	0.56
4	2000x8.96	26.21	346.2	413.8	50	0.8	1.22
5	2000x8.96	25.56	346.2	413.6	50	0.7	1.15
6	2000x8.96	24.16	346.2	413.6	50	0.7	1.15
7	2000x8.96	22.72	346.2	414.6	50	0.7	1.05
8	2000x8.96	20.86	346.2	413.1	50	0.8	1.06

9	2000x8.96	17.85	346.2	411.9	50	0.8	0.97
3	2250x15	18.32	351.6	425.5	50	0	1.08
4	2250x15	9.79	350.3	418.1	50	0.1	1.19
5	2250x15	11.20	350.5	422.6	50	0	1.51
6	2250x15	12.09	350.7	423.2	50	0	1.49
7	2250x15	13.83	350.9	423.5	50	0	1.4
8	2250x15	14.28	351	422.6	50	0	1.45
9	2250x15	15.21	351.1	422.2	50	0.1	0.99
10	2250x15	16.62	351.1	423.9	50	0	1.34

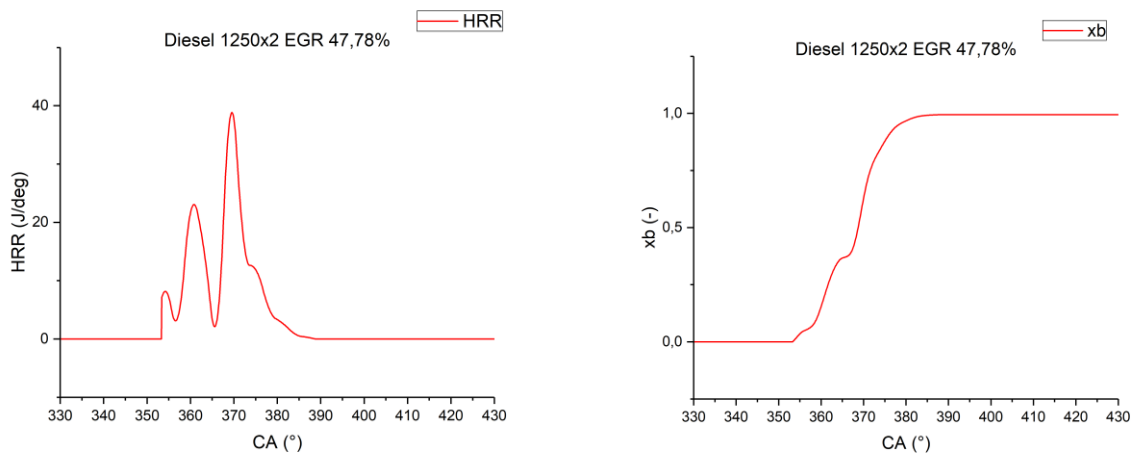
Table 4.2 Calibration results for tests conducted with HVO

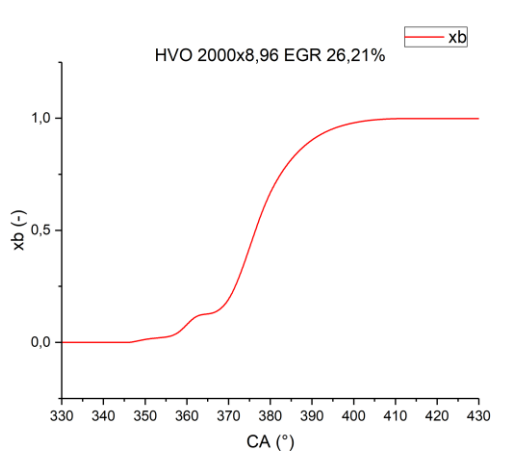
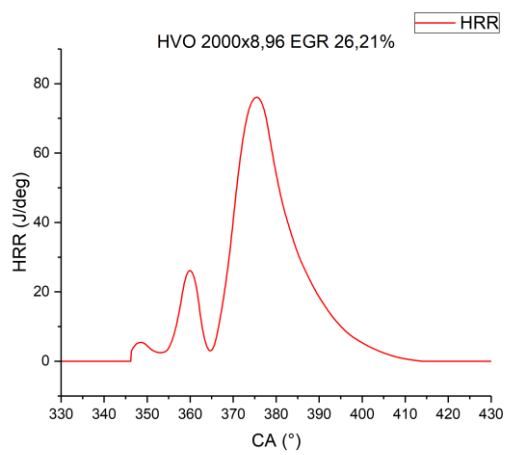
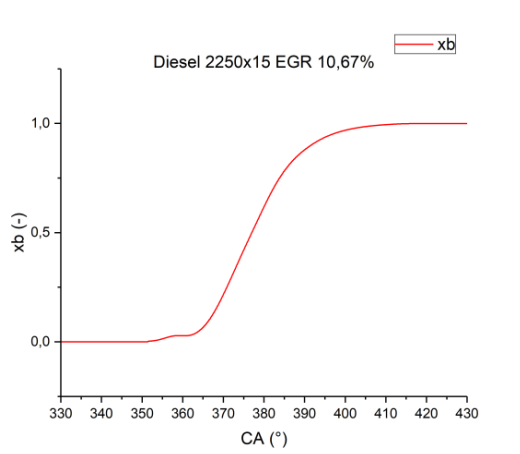
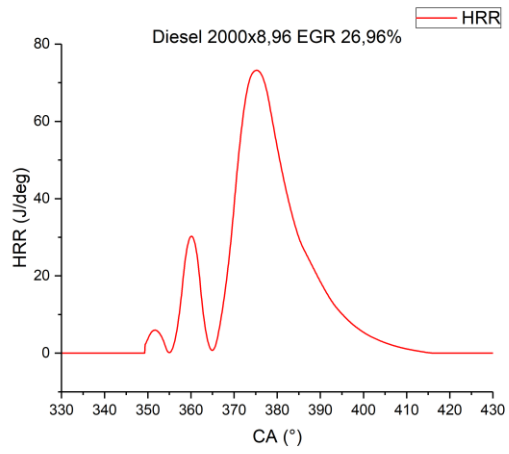
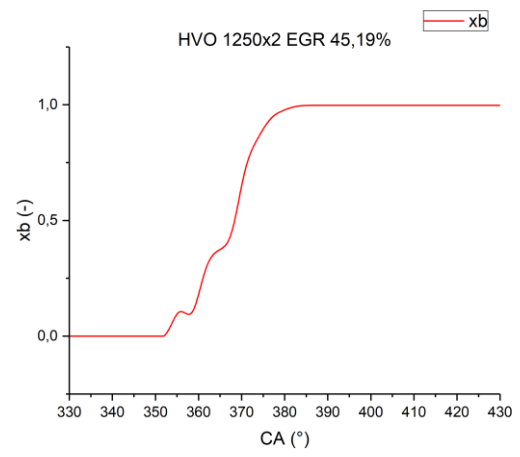
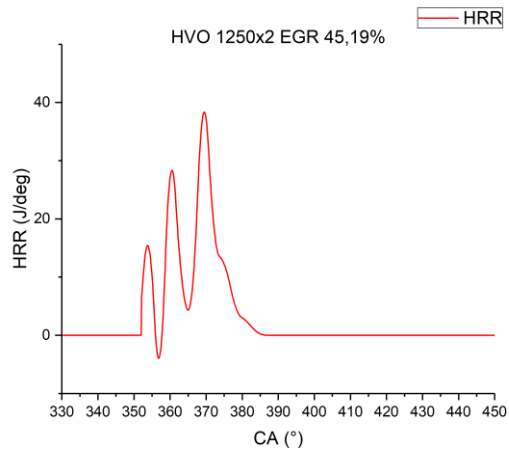
The first interesting output of the calibrated model is that all the tests conducted have a  $C_0$  of 50, so the fuel mass is underestimated for all the tests. In particular, tests conducted with HVO as fuel show a greater underestimation of the fuel quantity with respect the tests conducted with diesel.

For what concern the calibration of the first pilot injection, the tests conducted at higher load (2250x15) are the ones that never show adding quantities (with the exception of two test conducted with HVO, where the increment are really low).

Looking at the SOC values of the two tables, it is possible to see that the tests conducted with HVO show a lower ignition delay with respect the diesel ones (the injection timing is equal for both fuels).

### 4.3. Graphical result





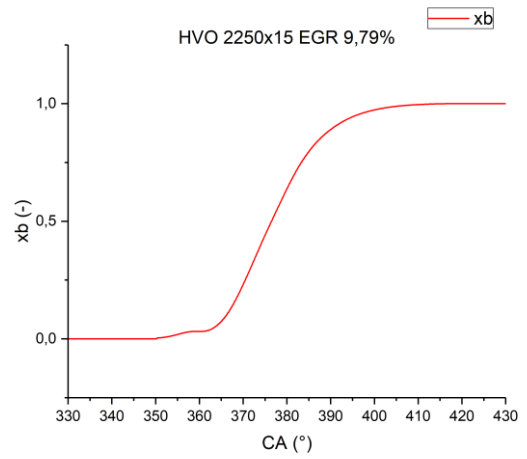
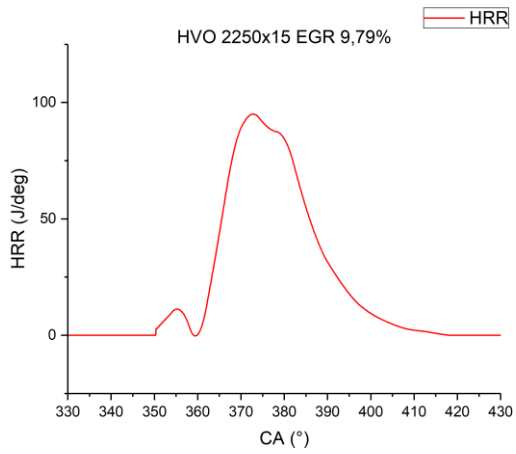
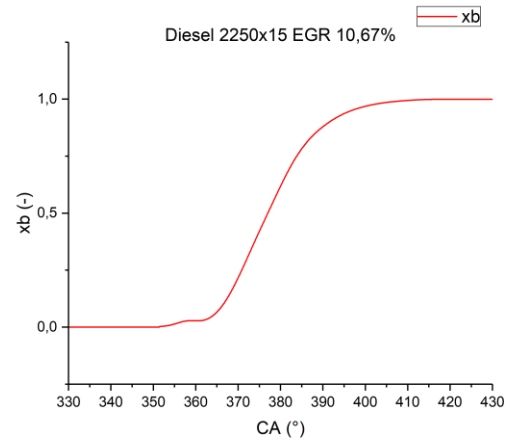
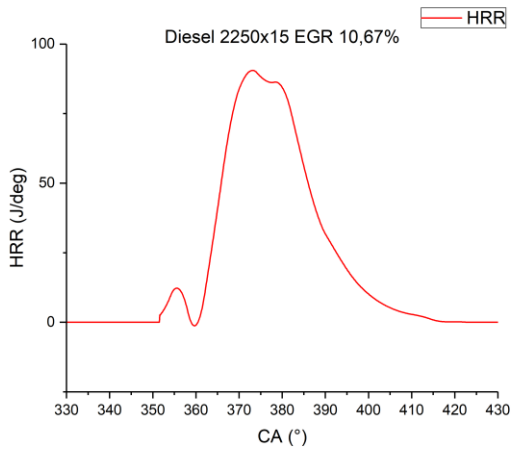


Figure 4.5 HRR curves (on the left) and mass fraction burned curves (on the right) for all working points and both fuels

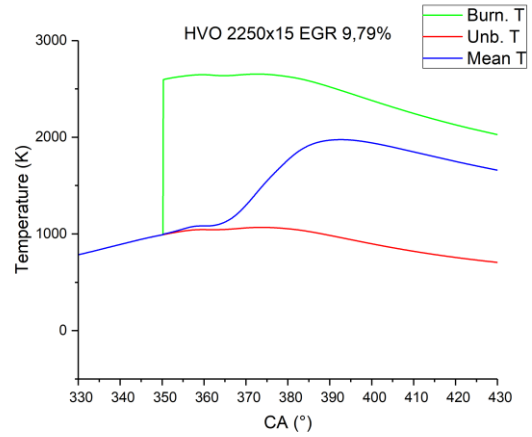
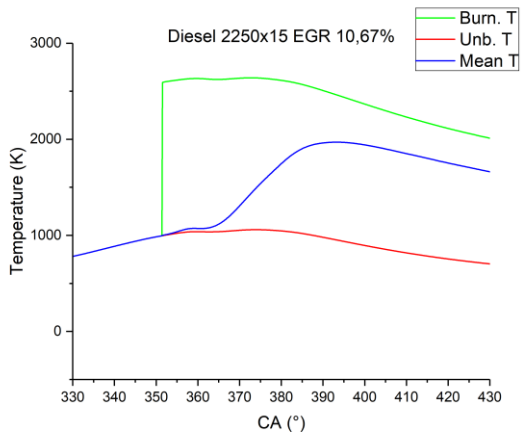
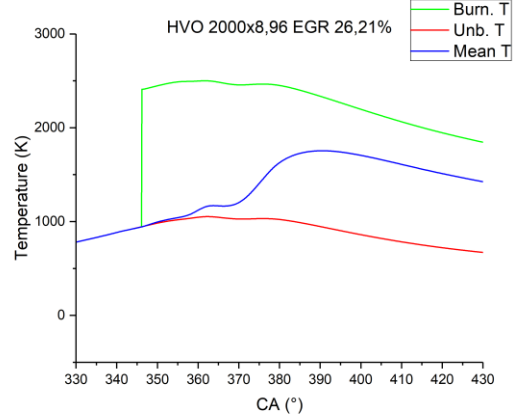
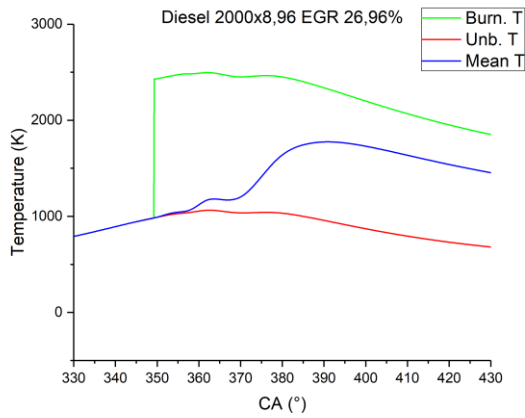
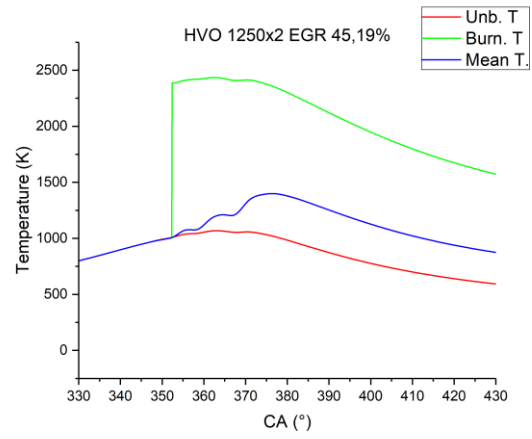
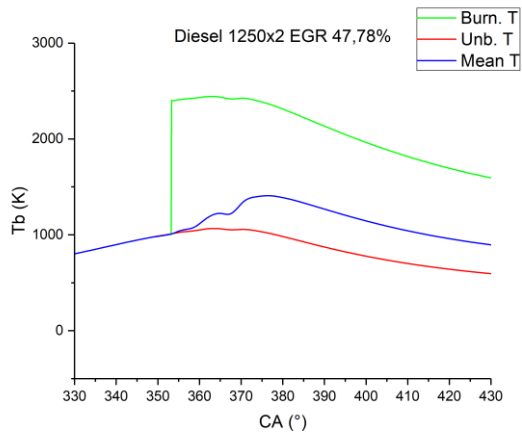


Figure 4.6 Temperature of the different zones

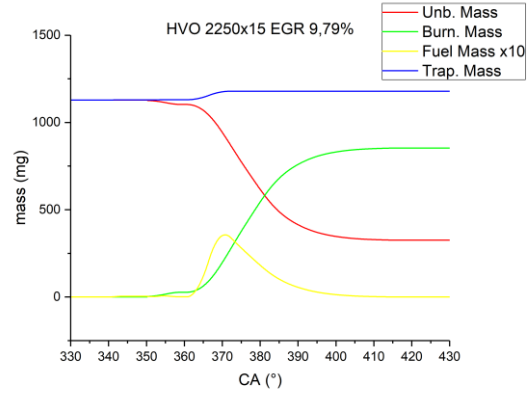
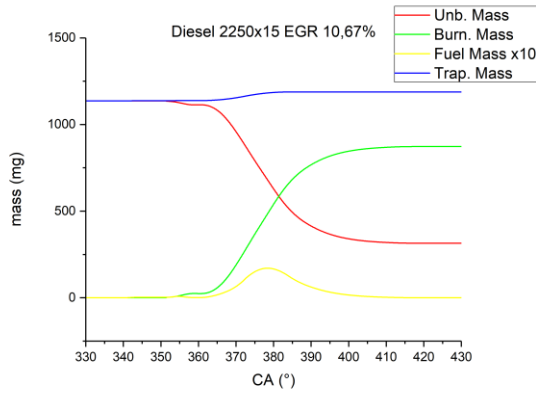
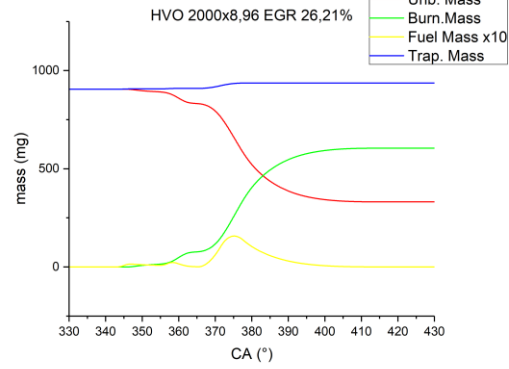
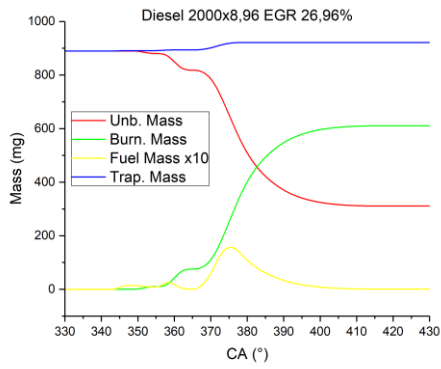
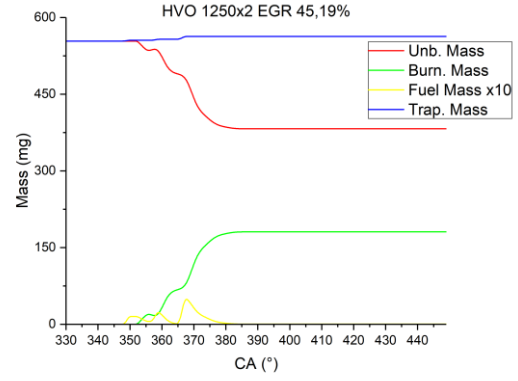
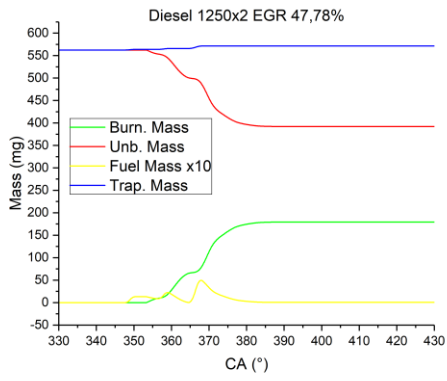
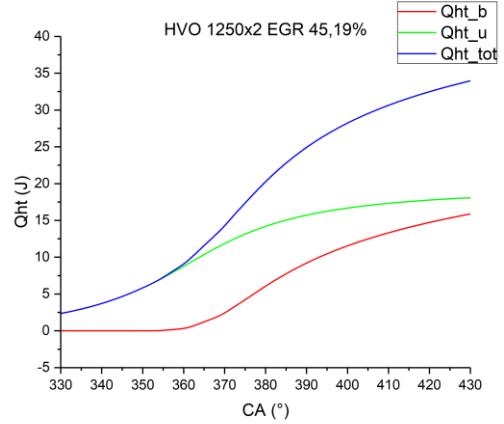
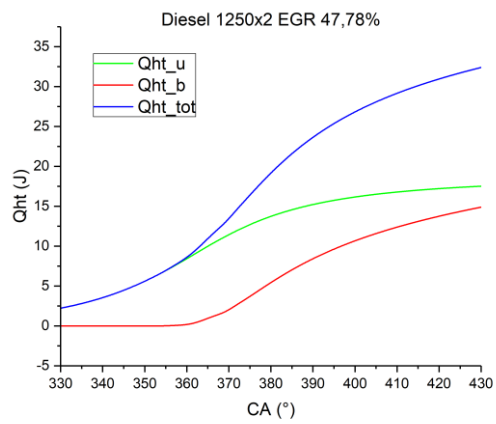


Figure 4.7 Masses of the different zones



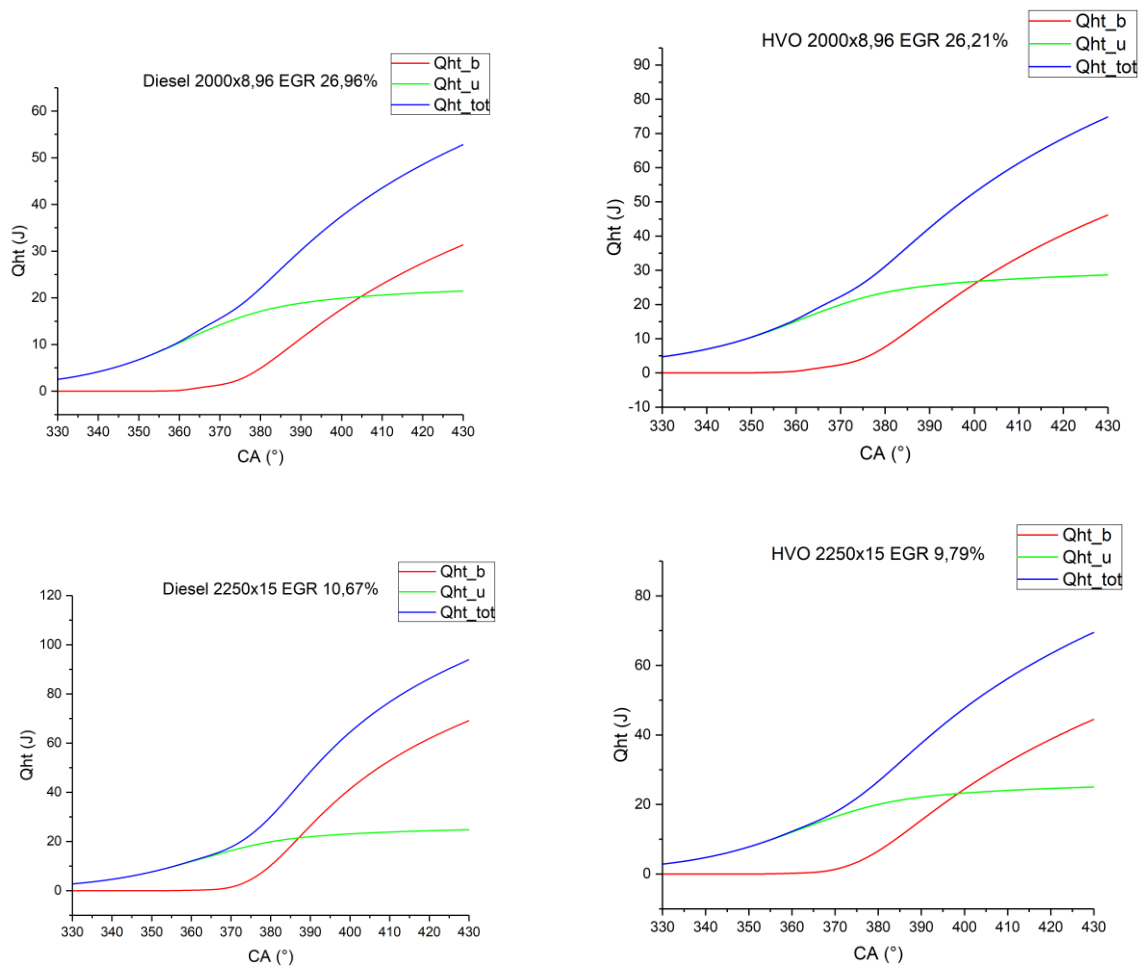


Figure 4.8 Heat transfer to the wall for the different working points

## 4.4. Comparison between Diesel and HVO

The comparison between tests conducted with diesel and the ones conducted with HVO is conducted considering the same injection timing and the same position of the EGR valve.

The comparison between tests is conducted considering three parameters: the cycle pressure, the temperature of the burned gas region, the mass fraction burned curve and the HRR curve. This graphs are reported below:

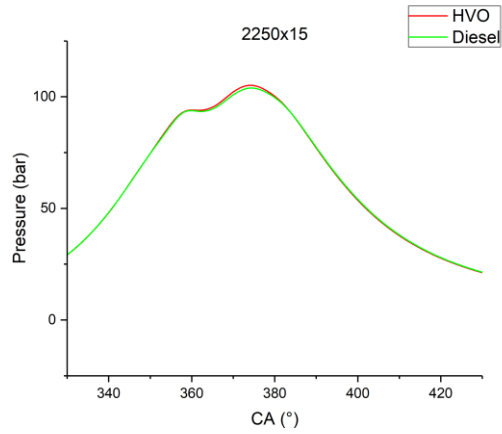
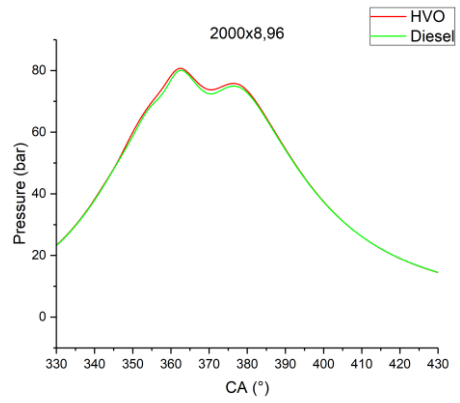
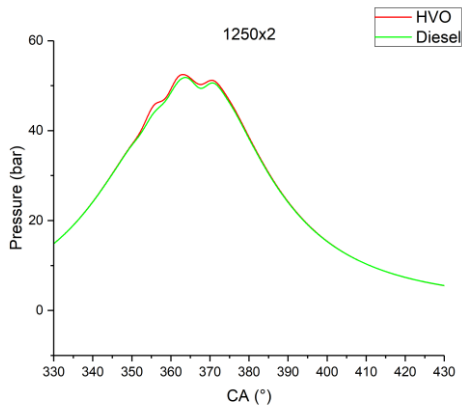
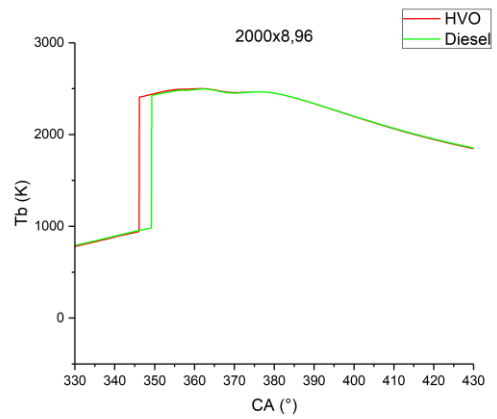
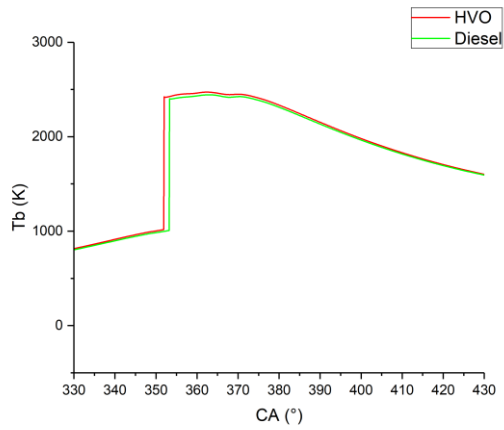


Figure 4.9 Pressure comparison at different working points



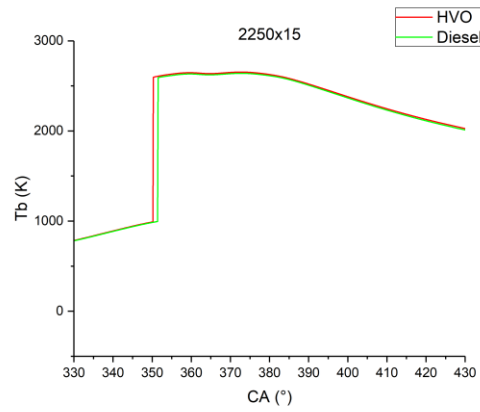


Figure 4.10 Burned zone temperature comparison for different working points

Looking at the temperature trends, it is possible to see that the HVO curve is rising up prior than the diesel one, that means that the HVO combustion has a lower ignition delay with respect the diesel one. This could be attributed to the fact that the tests conducted with HVO have a small difference in terms of EGR rate (from 0.5 to 2% less than the tests conducted with diesel).

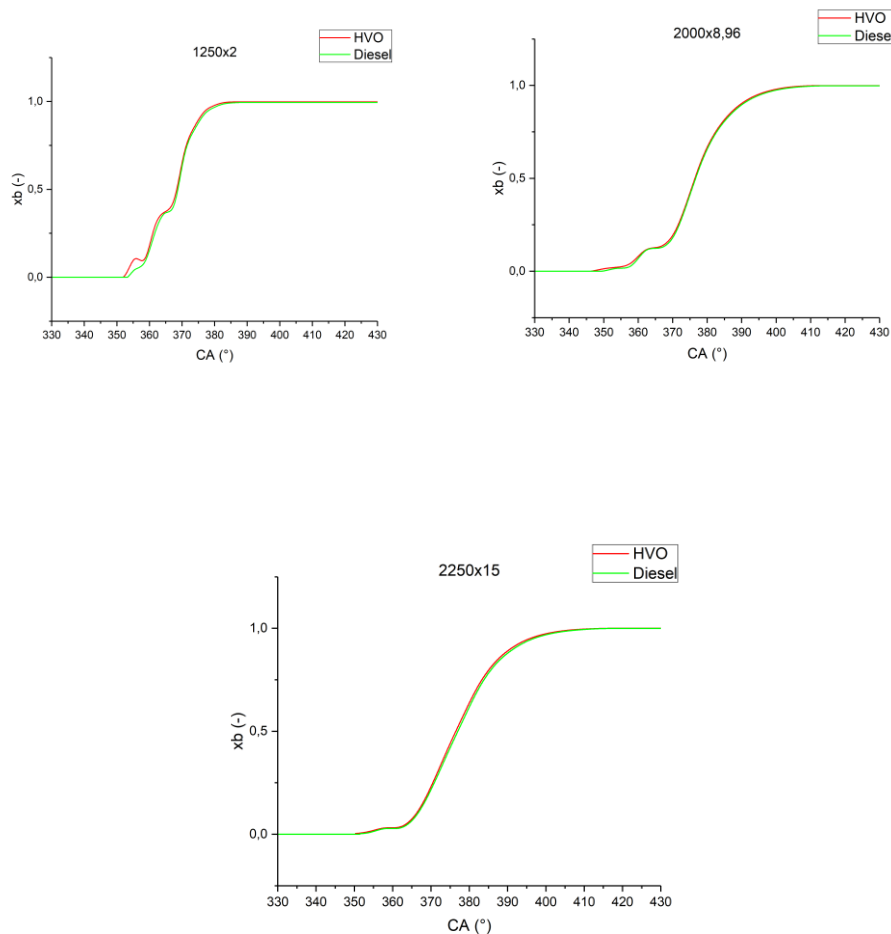


Figure 4.11 Comparison of the mass fraction burned curves for different working point

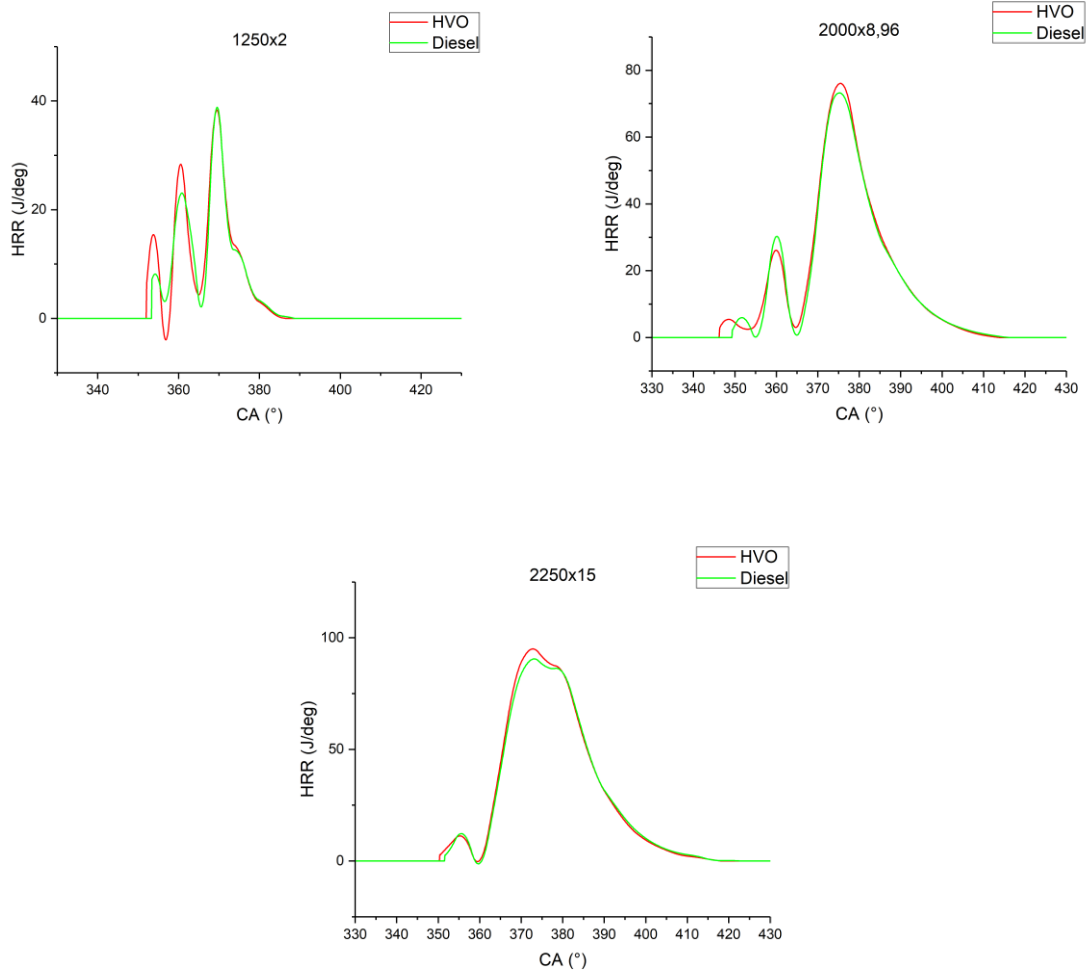


Figure 4.12 HRR curves comparison for different working points

From the above figure, it is possible to see that increasing the load, the peak value of the HRR curves for the HVO curve becomes greater and greater with respect the peak value of the diesel curve.

## 4.5. Comparison between one zone and three zone model

The comparison between the one zone model and the three zone model is done considering:

- HRR
- Mass fraction burned
- The gross heat transfer to the wall

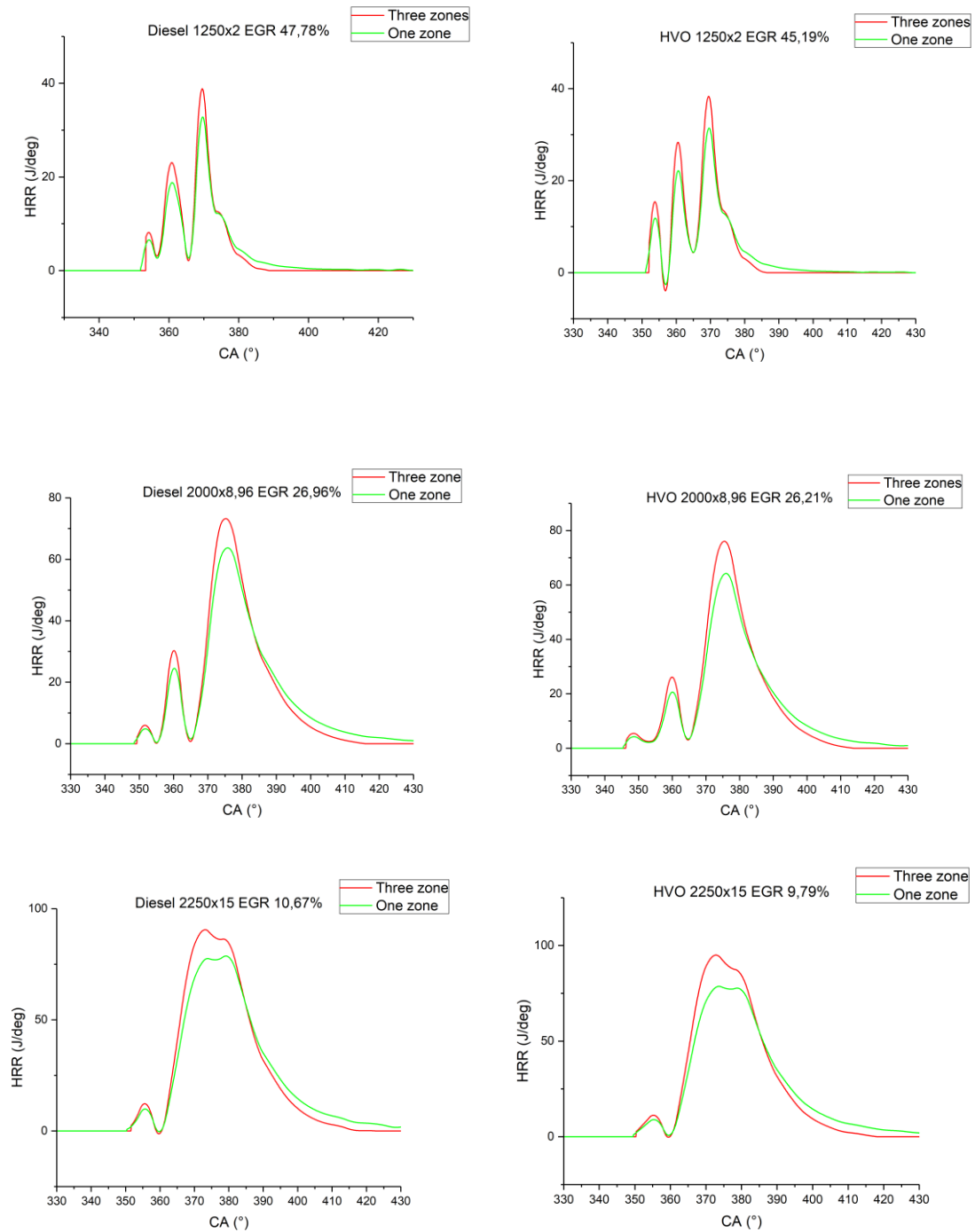


Figure 4.13 HRR trends according to the one zone model and to the three zones one

Looking at the above figure, it is possible to see that the two trends are very near at the beginning of the combustion (when burns the first pilot injection) and the greatest differences between the two curves could be seen in correspondence of the peaks. Moreover, it could be seen that increasing the load the two curves deviate earlier each other. For all the test conducted it is possible to say that the curve corresponding to the three zones model has higher peak value with respect to the one zone one. This means that in the three zone model there is an higher chemical energy release rate.

This trend is inverted after the peak of the curves. In fact, in this region the one zone model estimates an higher chemical energy release rate with respect the three zones one.

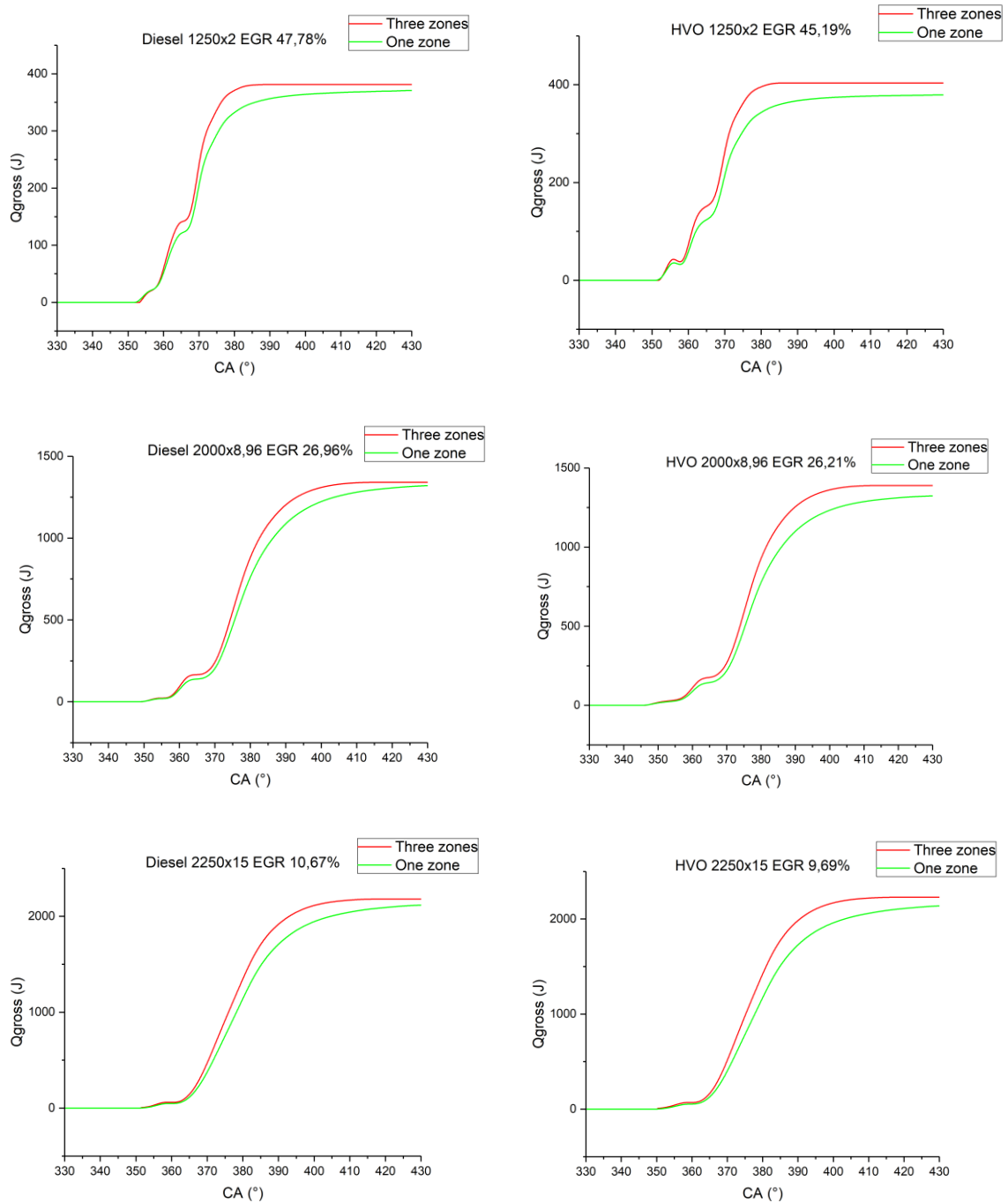


Figure 4.14  $Q_{gross}$  trends according to the one zone model and to the three zones one

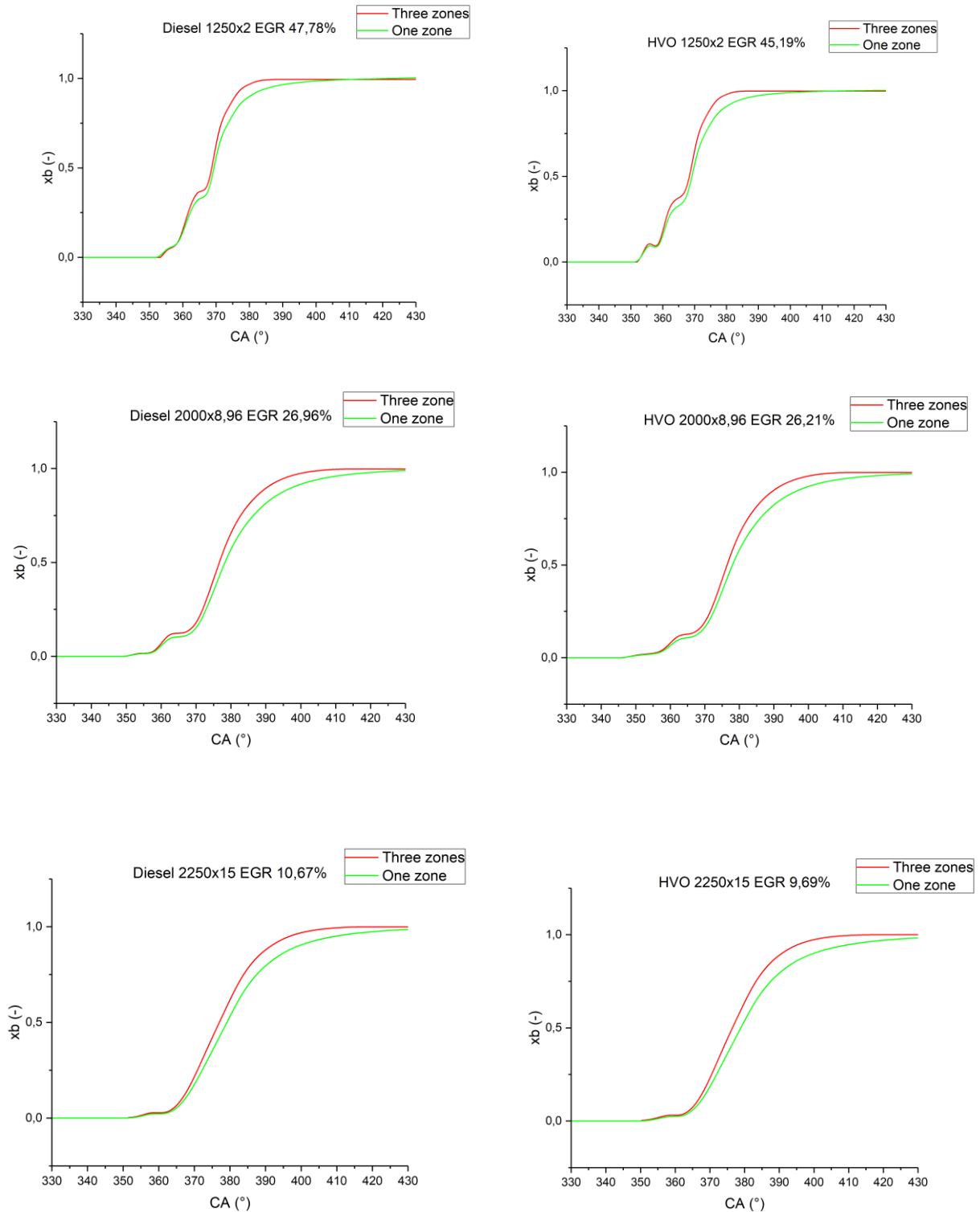


Figure 4.15  $x_b$  trends according to the one zone model and the three zones one

From *Figure 4.14* and *Figure 4.15* it is possible to say that the one zone model overestimate the combustion duration with respect the three zones one. The differences are between the curves are also given by the fact that in the three zones model the injected quantity is always underestimated, and so a fuel quantity is added

to the original one (looking at the gross heat transfer is it possible to see greater differences in the tests conducted with HVO since these tests requires an higher adding fuel quantity).

Pressure File	Engine Point	EGR rate [%]	MFB5	MFB10	MFB50	MFB90	MFB5_1Z	MFB10_1Z	MFB50_1Z	MFB90_1Z
32	1250x2	47.78	-3.96	-1.18	8.61	15.65	-4.43	-1.05	9.28	19.98
33	1250x2	50.83	-2.39	-0.67	9.03	16.02	-2.35	-0.41	9.70	20.37
34	1250x2	49.99	-2.53	-0.77	8.87	15.86	-2.51	-0.51	9.55	20.37
35	1250x2	48.11	-3.28	-1.09	8.66	15.71	-3.66	-0.93	9.32	19.98
36	1250x2	47.79	-3.74	-1.21	8.60	15.83	-4.23	-1.09	9.24	19.83
37	1250x2	47.91	-3.80	-1.10	8.64	15.69	-4.36	-0.98	9.29	19.96
38	1250x2	47.82	-3.81	-1.15	8.61	15.70	-4.34	-1.03	9.25	19.84
4	2000x8.96	26.96	-0.96	1.37	16.56	30.26	-0.44	3.16	18.17	37.55
5	2000x8.96	25.76	-0.98	1.47	16.56	30.25	-0.41	3.86	18.17	37.56
6	2000x8.96	23.99	-1.21	1.23	16.40	29.77	-0.60	3.12	18.02	37.09
7	2000x8.96	21.84	-1.22	1.32	16.33	29.57	-0.58	3.88	17.98	37.00
8	2000x8.96	19.21	-1.43	1.21	16.20	29.25	-0.76	3.77	17.87	36.68
9	2000x8.96	17.02	-1.57	1.10	16.08	28.89	-0.88	3.52	17.76	36.43
3	2250x15	19.52	4.23	6.76	17.72	33.41	4.93	7.59	19.73	41.30
4	2250x15	10.67	3.93	6.40	16.90	31.46	4.69	7.26	19.03	39.12
5	2250x15	12.49	3.98	6.47	17.08	31.96	4.75	7.34	19.21	39.81
6	2250x15	13.30	4.00	6.50	17.10	32.03	4.77	7.36	19.22	39.92
7	2250x15	15.21	4.06	6.55	17.25	32.48	4.81	7.41	19.34	40.36
8	2250x15	16.07	4.05	6.57	17.33	32.60	4.80	7.42	19.41	40.48
9	2250x15	16.73	4.11	6.63	17.45	32.85	4.85	7.49	19.49	40.54

	5									
10	2250x15	18.50	4.15	6.67	17.53	33.08	4.85	7.49	19.53	40.71

Table 4.3 Combustion metrics comparison between one zone model and three zones one using diesel

Pressure File	Engine Point	EGR rate [%]	MFB5	MFB10	MFB50	MFB90	MFB5_1Z	MFB10_1Z	MFB50_1Z	MFB90_1Z
32	1250x2	45.19	-6.43	-1.45	8.27	15.08	-6.27	-1.33	9.07	19.25
33	1250x2	48.68	-6.03	-1.27	8.67	15.30	-5.92	-0.99	9.41	19.60
34	1250x2	47.52	-6.18	-1.54	8.47	15.17	-6.10	-1.25	9.20	19.14
35	1250x2	45.50	-6.28	-4.22	8.38	15.07	-6.16	-1.17	9.17	19.50
36	1250x2	45.04	-6.46	-1.91	8.27	15.06	-6.29	-1.40	9.06	19.21
37	1250x2	45.19	-6.45	-1.81	8.27	15.03	-6.28	-1.34	9.08	19.32
38	1250x2	45.16	-6.44	-1.87	8.25	15.08	-6.27	-1.33	9.06	19.36
4	2000x8.96	26.21	-1.77	1.05	16.34	29.69	-1.14	2.72	17.90	36.65
5	2000x8.96	25.56	-1.80	1.02	16.30	29.63	-1.16	2.69	17.88	36.75
6	2000x8.96	24.16	-1.88	0.99	16.19	29.32	-1.24	2.70	17.77	36.42
7	2000x8.96	22.72	-1.98	0.93	16.15	29.26	-1.33	2.64	17.77	36.53
8	2000x8.96	20.86	-2.05	0.90	16.05	29.02	-1.39	2.66	17.67	36.32
9	2000x8.96	17.85	-2.14	0.83	15.91	28.48	-1.46	2.57	17.55	35.82
3	2250x15	18.32	3.80	6.43	17.22	32.91	4.50	7.23	19.38	41.68
4	2250x15	9.79	3.44	6.05	16.38	30.65	4.30	6.96	18.81	39.78
5	2250x15	11.20	3.62	6.19	16.67	31.49	4.39	7.05	19.00	40.39
6	2250x15	12.09	3.63	6.23	16.71	31.50	4.40	7.07	18.98	40.05
7	2250x15	13.83	3.70	6.28	16.88	31.97	4.45	7.12	19.13	40.82
8	2250x15	14.28	3.70	6.30	16.88	31.88	4.44	7.12	19.08	40.28

9	2250x15	15.21	3.59	6.26	16.86	31.80	4.43	7.15	19.20	40.92
10	2250x15	16.62	3.69	6.35	17.05	32.34	4.44	7.17	19.21	40.72

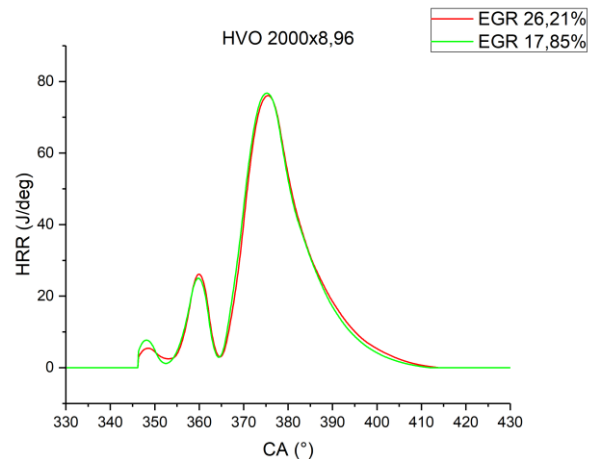
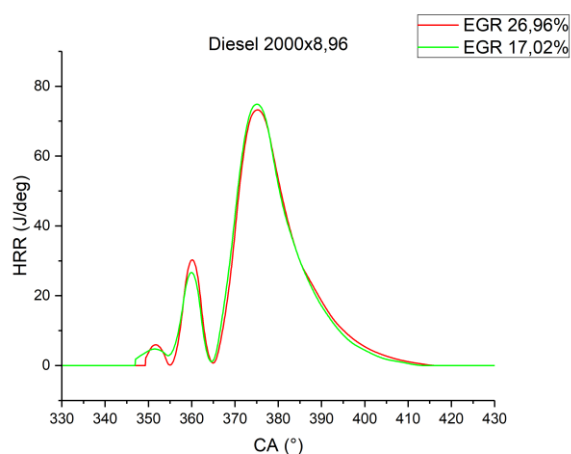
Table 4.4 Combustion metrics comparison between one zone model and three zones one

From the two tables above, it is possible to say that the initial part of the combustion (MFB5 and MFB10) are very similar between one zone model and three zones one. At lower load also MFB50 is well estimated by the one zone model, while MFB90 demonstrates that the one zone model overestimates the combustion duration.

## 4.6. EGR effects

In order to understand how EGR influences the main combustion parameters, several tests are conducted for the same engine working point varying the quantity of recirculated gases through the action on the EGR valve. Reducing the EGR quantity means to increase the oxygen concentration inside the combustion chamber and so, in order to keep constant the bmep, it is required to slightly decrease the quantity of the injected fuel. The EGR influence is evaluated on:

- HRR curves
- Mass fraction burned
- Burning temperature



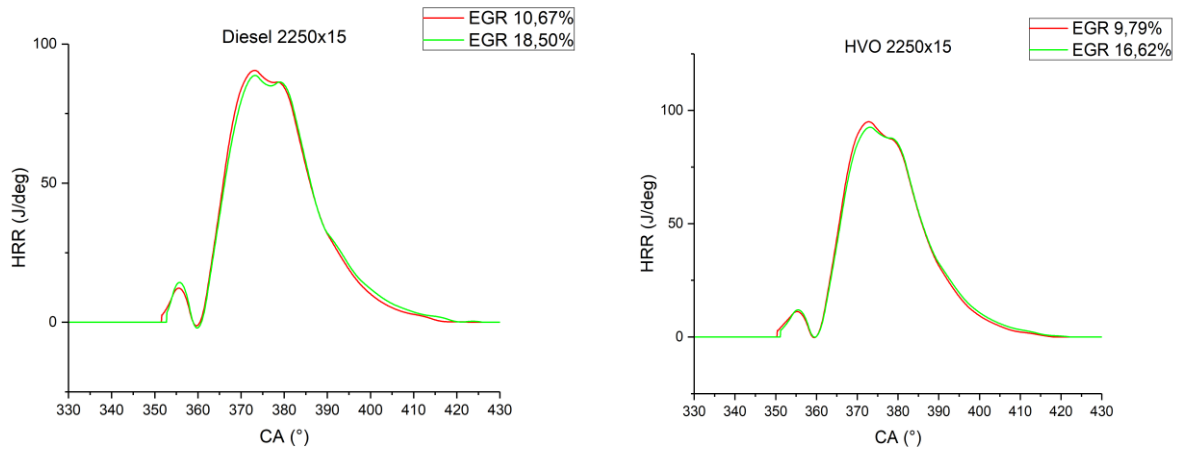


Figure 4.16 EGR effects on HRR

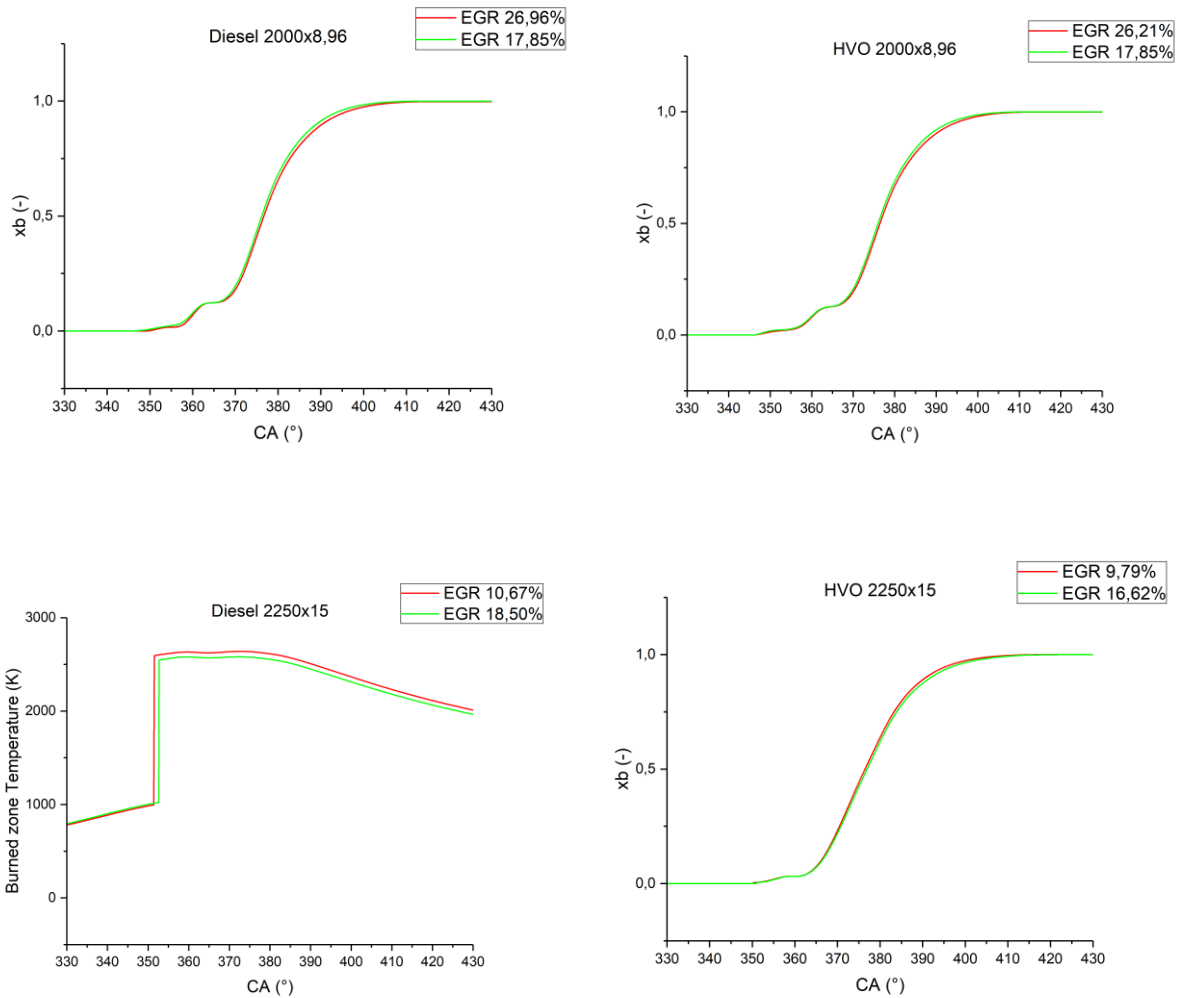


Figure 4.17 EGR effects on xb

From the above figures it is possible to see that increasing the percentage of EGR means to lower the peaks of the heat release rate curve and to shift of a little angle the peaks of the HRR curve toward greater crank angle. This occurs because increasing the EGR rate means to introduce yet burned gases that lower the reactivity of the mixture and, in turns, they increase the ignition delay.

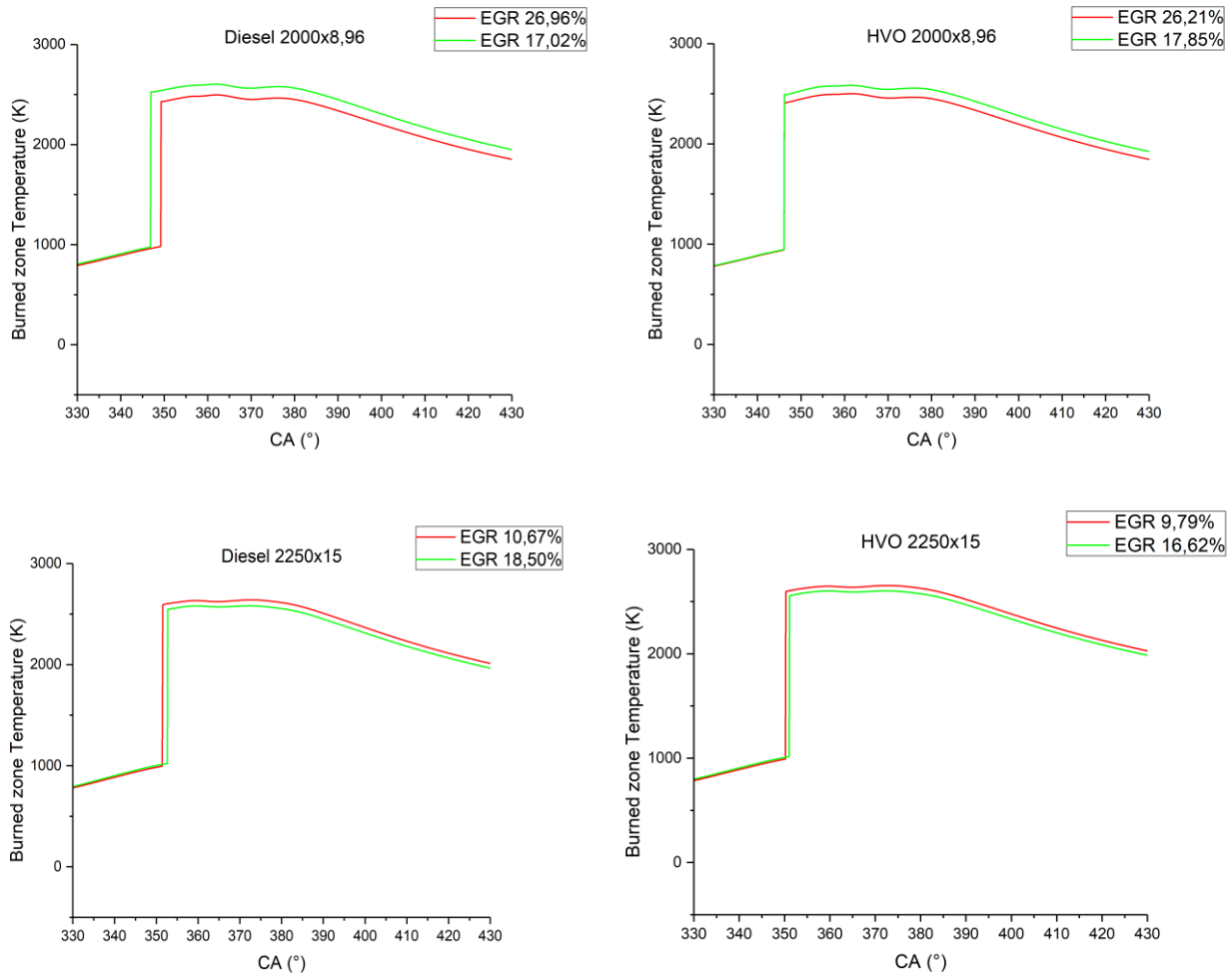


Figure 4.18 EGR effects on the burned zone temperature

The general trend of the burned zone temperature is to decrease while increasing the EGR rate. This is mainly due to the thermic effect of the EGR gases. In fact, the exhaust gases have an higher heat capacity with respect the fresh air, and so they are able to absorb a greater quantity of heat.

## 5. Submodel for NO<sub>x</sub> formation

The submodel that this work is going to use is estimating only NO concentration, not considering the NO<sub>2</sub> one. This hypothesis could limit the potentialities of the analysis, since for a diesel engine the emission of NO<sub>2</sub> could reach the 30% of the total NO<sub>x</sub> emission.

For this model the Zeldovich formation mechanism and the prompt one are considered. Starting from the Zeldovich mechanism, only the first three reactions are taken into account:



The idea behind this model is to use the kinetic model in order to evaluate the formation ratio of NO. If the first reaction is considered:

$$\frac{d[NO]}{dt} = k_1^+ [N_2]_e [O]_e - k_1^- [NO][N] \quad Eq. 54$$

Where  $k$  is the reaction rate constant, defined using the exponential correlation of Arrhenius:

$$k = aT^b e^{-\frac{A}{RT}} \quad Eq. 55$$

Considering the other two reaction of the Zeldovich mechanism and mixing it together, the following expression is obtained:

$$\frac{d[NO]_b}{dt} = \frac{\zeta k_1^+ * 2 \left[ 1 - \left( \frac{[NO]_b}{[NO]_{b,e}} \right)^2 \right] [N_2]_{b,e} [O]_{b,e}}{1 + \left( \frac{[NO]_b}{[NO]_{b,e}} \right) \frac{k_1^+ [N_2]_{b,e} [O]_{b,e}}{k_2^- [NO]_{b,e} [O]_{b,e} + k_3^- [NO]_{b,e} [H]_{b,e}}} \quad Eq. 56$$

Where  $\zeta$  is the calibration parameter. The automatic calibration procedure consists in have as output of the model a final NO concentration that is in the neighbourhood of the measured one. A threshold of 3 ppm was fixed and two extreme values of the calibration parameter, that are 0 and 2.

The quantities inside the square brackets are the concentration of the species. The concentration characterized by the subscript  $e$  are obtained by tables as function pressure and temperature.

The three reaction rate constants that are present in the above expression are quantified by Miller expressions [2]:

$$k_1^+ = 1.8 * 10^{14} e^{\left(-\frac{38370}{T_b}\right)} \quad Eq. 57$$

$$k_2^- = \frac{1.8 * 10^{10} e^{\left(-\frac{4680}{T_b}\right)}}{10^{0.7691 \log(T_b) + 0.7109 * \frac{10^4}{T_b} - 4.0366 - 3.9154 * 10^{-4} * T_b + 0.0718 * 10^{-6} T_b^2}} \quad Eq. 58$$

$$k_3^- = \frac{7.1 * 10^{13} e^{\left(-\frac{450}{T_b}\right)}}{10^{0.5383 \log(T_b) + 1.0723 * \frac{10^4}{T_b} - 4.0366 - 3.9154 * 10^{-4} * T_b + 0.0427 * 10^{-6} T_b^2}} \quad Eq. 59$$

Knowing the expression of the time derivative of the NO, now it is possible to write the equation that describes the instantaneous concentration of NO in the cylinder:

$$[NO]_b^{t+dt} + V_b^{t+dt} = [NO]_b^t + V_b^t + \frac{d[NO]_b}{dt} dt V_b^{t+dt} + dn_{NO,b,in} - dn_{NO,b,out} \quad Eq. 60$$

This model does not consider exiting moles of NO from the burned gases, while the entering one are the sum of the prompt mechanism and the ones that enter into the burning zone.

$$dn_{NO,b,in} = \langle NO \rangle_u \frac{dm_{u \rightarrow b}}{M_u} + \langle NO \rangle_{prompt} \frac{dm_b}{M_b} \quad Eq. 61$$

The concentration in the triangular brackets are no dimensional concentration indicated with the molar fraction.

The concentration of the NO produced according with the prompt mechanism are obtained fitting the Fenimore curve with a polynomial correlation that is function of the equivalence ratio.

$$\langle NO \rangle_{prompt} = 10^{\log\left(\frac{[NO]}{[NO]_e}\right)} \langle NO \rangle_{e,prompt} \quad Eq. 62$$

For what regards the concentration of NO in the unburned gases, the previous thesis student applies a two-step procedure [8]. In the first step it was assumed that the concentration of the unburned gases NO is null and a first attempt concentration of NO was calculated using the following formula:

$$\langle \overline{NO} \rangle_{first} = \frac{n_{NO,b}}{n_{tot}} \quad Eq. 63$$

Then the unburned gases NO concentration could be determined:

$$\langle NO \rangle_u = \frac{\langle \overline{NO} \rangle_{first} \frac{(m_{res} + m_{EGR})}{M_b}}{\frac{m_{air} + m_{res} + m_{EGR}}{M_u}} \quad Eq. 64$$

Then the total iterative process continues until the difference between the above concentration and the one that is present in the Eq.61 is lower than  $10^{-6}$ . The results of the calibration process are reported below.

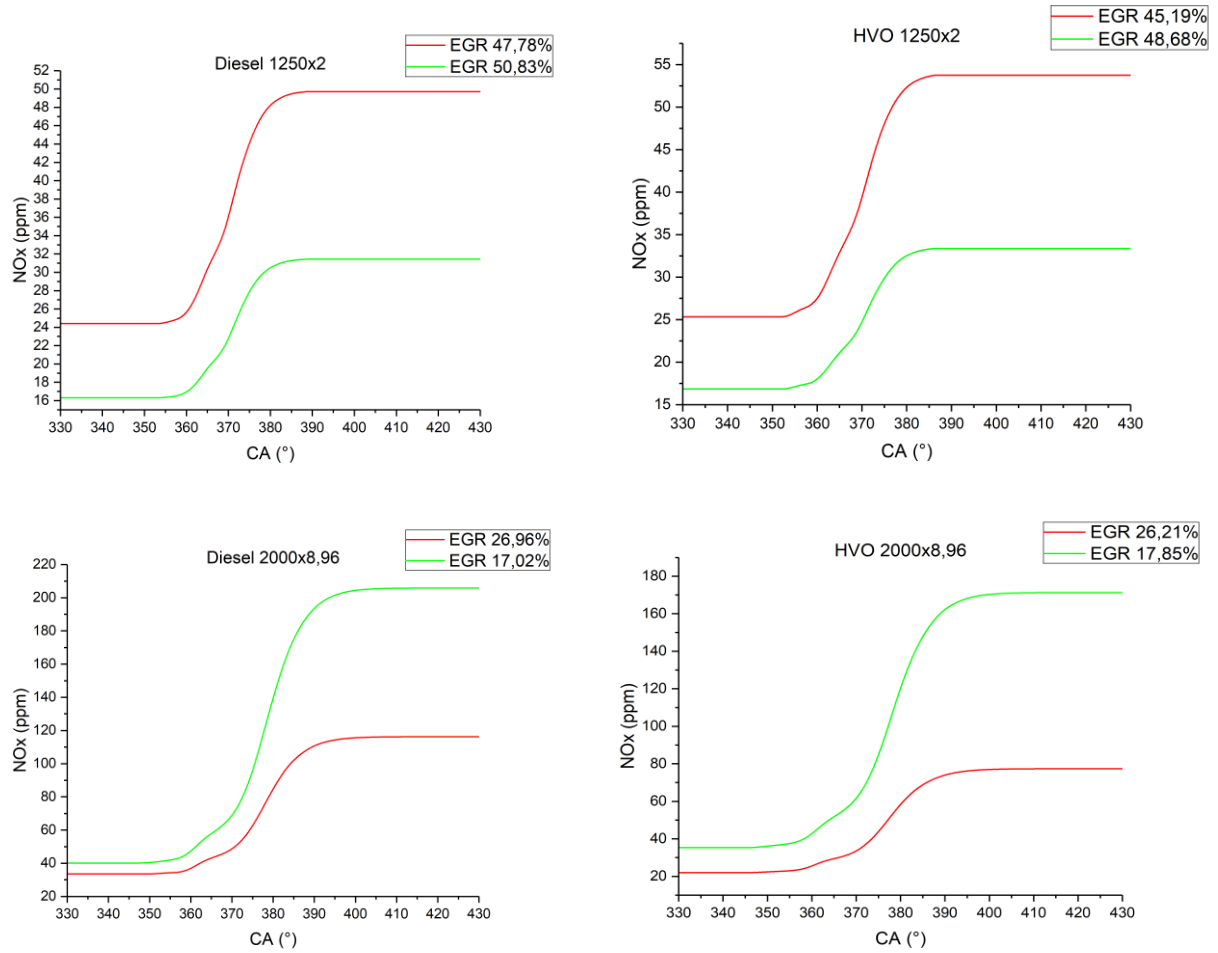
Pressure File	Engine Point	EGR rate [%]	$\zeta$
32	1250x2	47.78	0.080
33	1250x2	50.83	0.084
34	1250x2	49.99	0.078
35	1250x2	48.11	0.078
36	1250x2	47.79	0.055
37	1250x2	47.91	0.068
38	1250x2	47.82	0.082
4	2000x8.96	26.96	0.081
5	2000x8.96	25.76	0.056
6	2000x8.96	23.99	0.050
7	2000x8.96	21.84	0.048
8	2000x8.96	19.21	0.044
9	2000x8.96	17.02	0.042
3	2250x15	19.52	0.064
4	2250x15	10.67	0.048
5	2250x15	12.49	0.046
6	2250x15	13.30	0.043
7	2250x15	15.21	0.043
8	2250x15	16.07	0.040
9	2250x15	16.73	0.033
10	2250x15	18.50	0.035

*Table 5.1 Calibration results for tests with diesel*

Pressure File	Engine Point	EGR rate [%]	$\zeta$
32	1250x2	45.19	0.059
33	1250x2	48.68	0.057
34	1250x2	47.52	0.059
35	1250x2	45.50	0.053
36	1250x2	45.04	0.061
37	1250x2	45.19	0.060
38	1250x2	45.16	0.059
4	2000x8.96	26.21	0.042
5	2000x8.96	25.56	0.037
6	2000x8.96	24.16	0.036
7	2000x8.96	22.72	0.037
8	2000x8.96	20.86	0.039
9	2000x8.96	17.85	0.043
3	2250x15	18.32	0.039
4	2250x15	9.79	0.038
5	2250x15	11.20	0.041
6	2250x15	12.09	0.043
7	2250x15	13.83	0.043
8	2250x15	14.28	0.039
9	2250x15	15.21	0.029
10	2250x15	16.62	0.035

Table 5.2 Calibration results for tests with HVO

Graphical results of the NO<sub>x</sub> formation model are reported below, with two different values of EGR for each test.



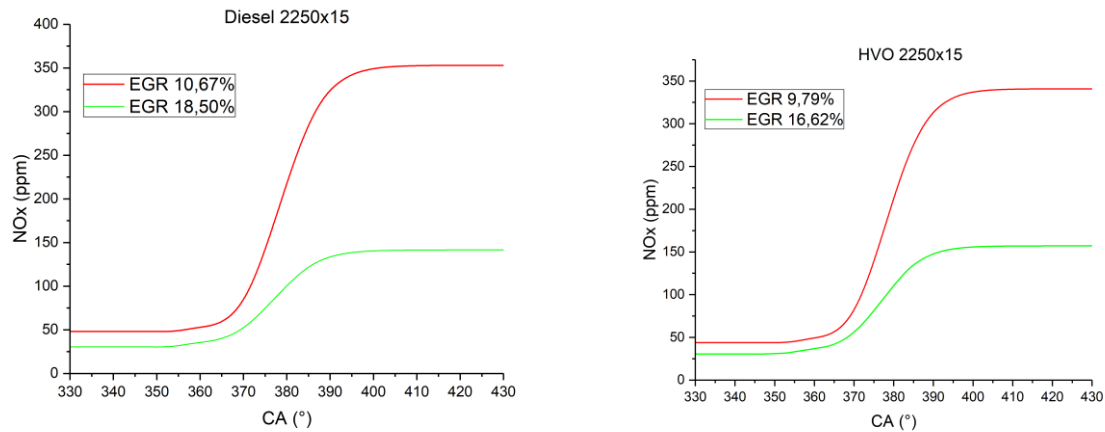
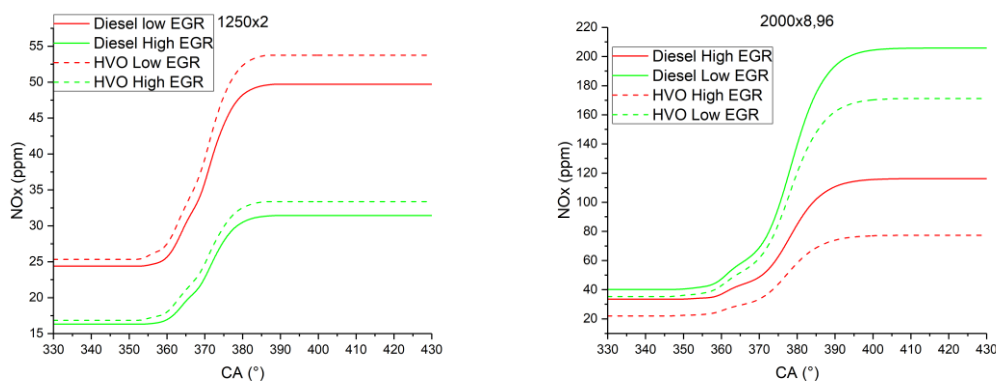


Figure 5.1 EGR effects on NO<sub>x</sub>

From the above figure all the trends seem to be coherent: in fact, increasing the percentage of recirculated gases it is possible to strongly lower the NO<sub>x</sub> emission. In order to decrease massively the NO<sub>x</sub> is not needed to work with high EGR level at high load. This could be explained looking at the exhaust composition: at low load the engine runs with an high air/fuel ratio, so the exhaust gases are plenty of oxygen. The oxygen does not participate to the dilution effect such as H<sub>2</sub>O and CO<sub>2</sub>, so an high EGR rate is needed in order to have a proper dilution. At high load, the exhaust gases have a poor content of oxygen, so a lower EGR rate is sufficient to reduce NO<sub>x</sub> emission. It is also possible to see that the concentration of NO<sub>x</sub> remains uncharged starting from 400° (40 aTDC), where temperature starts to be lower than 2000 K.

In order to understand the influence of the fuel in NO<sub>x</sub> emission, a comparative graph was done for each working point.



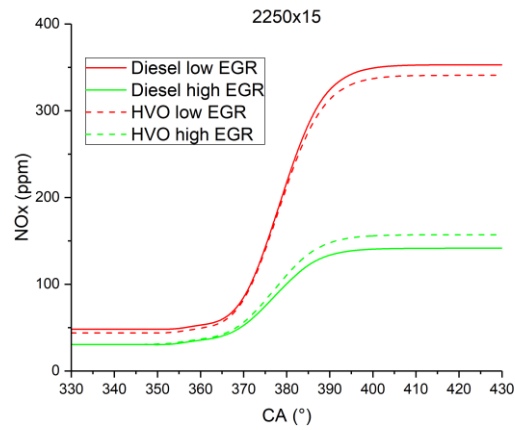


Figure 5.2 Fuel comparison with two EGR levels

Looking at the figure, there is not an univocal trend. In fact, at low load the tests done using HVO show higher level of NO<sub>x</sub> emission for both high/low EGR rate. For medium load HVO tests show lower NO<sub>x</sub> emission with respect diesel one for both high/low EGR rate. At high load there is an intermediate situation, with lower emission at low EGR rate and greater emission at high EGR rate.

## 6. Submodel for PM formation

Since the difficulty of the problem of PM formation (it is hard to estimate the composition of the soot), the model is only able to approximate the trend of soot inside the cylinder. Moreover, the three zones model used in not providing any submodel per the premixed phase, where the greatest part of soot is forming, but since the richer is the mixture the higher are PM emission, the model is able to partially capture the formation mechanism.

The submodel used for the formation mechanism is composed by two models:

- A formation model (Hyroyasu [12])
- An oxidation model (Nagle and Strickland-Constable)

The expression of the formation model is the following:

$$\frac{dm_{s,f}}{dt} = A_f p^{0.5} e^{-\frac{E_f}{RT_b}} m_{f,v} \quad Eq. 65$$

Where  $A_f$  is a pre-exponential Arrhenius constant and it is the calibrating parameter.  $E_f$  is the activation energy and it is equal to 12500 cal/mol.  $m_{f,v}$  is the mass of vaporized fuel, that is equal to the fuel mass since there are not vaporizing model.

The oxidation model has the following expression:

$$\frac{dm_{s,o}}{st} = \frac{6m_s}{\rho_s D_s} M_c R_{tot} \quad Eq. 66$$

Where  $\rho_s$  is the soot density,  $D_s$  is the diameter of the soot particle,  $M_c$  the molecular mass of the carbon and  $R_{tot}$  is the soot mass oxidate per time and per surface, that is defined by the following expression [2]:

$$R_{tot} = \frac{k_A p_{O_2}}{1 + k_z p_{O_2}} x + k_B p_{O_2} (1 - x) \quad Eq. 67$$

Where  $x$  is the surface fraction occupied by A sites, that are the most reactive one. This fraction is described by the following expression:

$$x = \left( 1 + \frac{k_T}{k_b p_{O_2}} \right)^{-1} \quad Eq. 68$$

The constants identified with  $k$  are function of the temperature, according to the following relations:

$$k_A = 20 e^{-\frac{15000}{T_b}} \quad Eq. 69$$

$$k_B = 4.46 * 10^{-3} e^{\left(-\frac{7640}{T_b}\right)} \quad Eq. 70$$

$$k_T = 1.51 * 10^5 e^{-\frac{48800}{T_b}} \quad \text{Eq. 71}$$

$$k_Z = 21.3 e^{\frac{2060}{T_b}} \quad \text{Eq. 72}$$

The mass of soot that is present in the cylinder crank angle by crank angle is the difference between the formed mass and the oxidated one. This two masses are the integrals of the equations 65 and 66.

Results of calibration are reported below:

Pressure File	Engine Point	EGR rate [%]	Af
32	1250x2	47.78	455
33	1250x2	50.83	305
34	1250x2	49.99	350
35	1250x2	48.11	415
36	1250x2	47.79	420
37	1250x2	47.91	470
38	1250x2	47.82	505
4	2000x8.96	26.96	2045
5	2000x8.96	25.76	2170
6	2000x8.96	23.99	2735
7	2000x8.96	21.84	2555
8	2000x8.96	19.21	2760
9	2000x8.96	17.02	2980
3	2250x15	19.52	1270
4	2250x15	10.67	1365
5	2250x15	12.49	870
6	2250x15	13.30	745
7	2250x15	15.21	870
8	2250x15	16.07	1600

9	2250x15	16.73	1620
10	2250x15	18.50	1405

*Table 6.1 Calibrations results for diesel tests*

Pressure File	Engine Point	EGR rate [%]	Af
32	1250x2	45.19	460
33	1250x2	48.68	345
34	1250x2	47.52	345
35	1250x2	45.50	475
36	1250x2	45.04	375
37	1250x2	45.19	515
38	1250x2	45.16	455
4	2000x8.96	26.21	1400
5	2000x8.96	25.56	1370
6	2000x8.96	24.16	1310
7	2000x8.96	22.72	1725
8	2000x8.96	20.86	1515
9	2000x8.96	17.85	1610
3	2250x15	18.32	955
4	2250x15	9.79	1160
5	2250x15	11.20	890
6	2250x15	12.09	1095
7	2250x15	13.83	925
8	2250x15	14.28	900
9	2250x15	15.21	1610
10	2250x15	16.62	1020

Table 6.2 Calibration results for HVO tests

Now some graphical results will be reported:

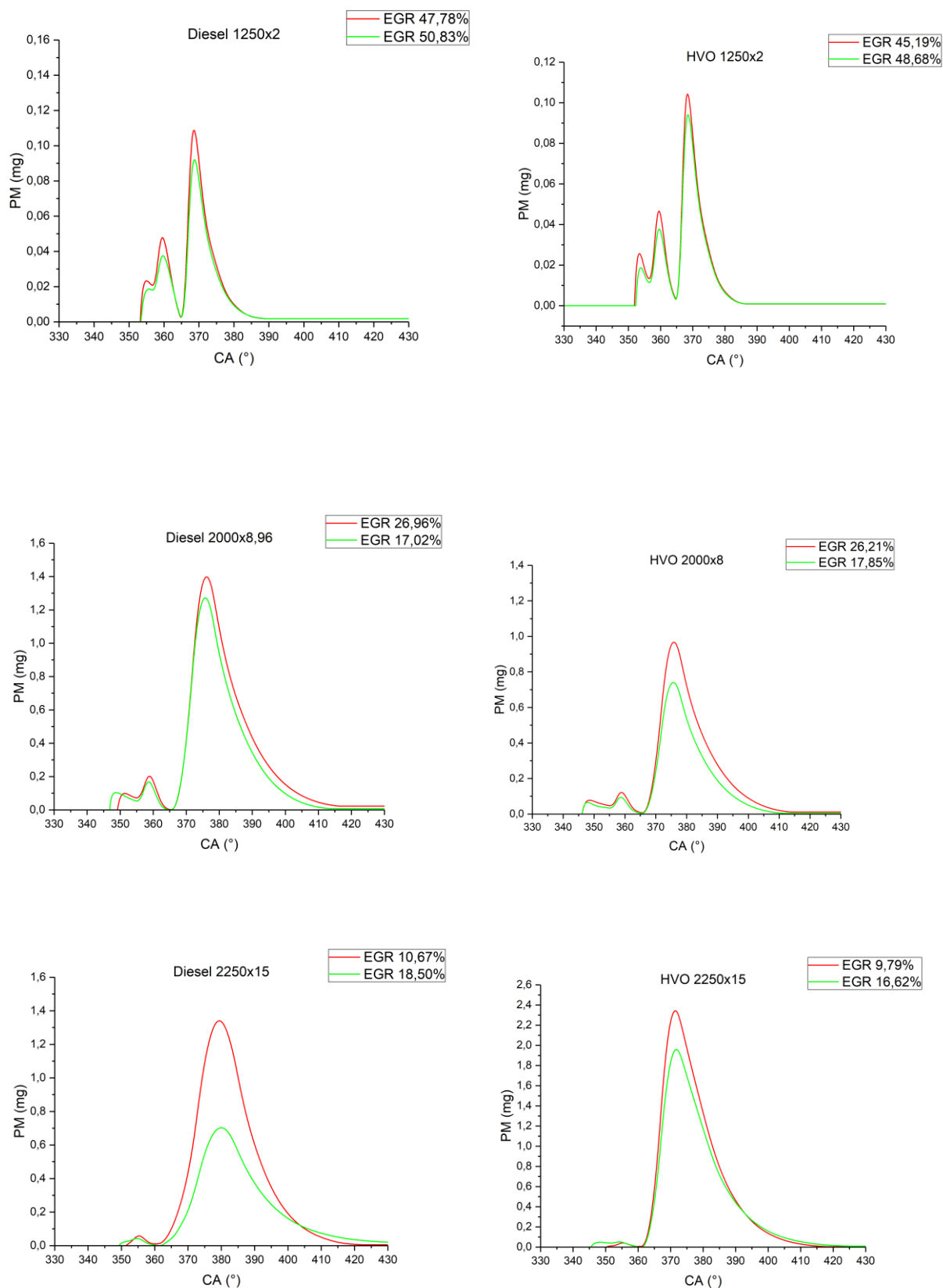


Figure 6.1 PM trends for all working point with two EGR level

For low load condition, the increasing of EGR level is not so detrimental for the PM emission. This is a condition that makes the behaviour of this working point closer to a PCCI engine, where the traditional trade-off between soot and NO<sub>x</sub> is missing [13].

For the other working points, the trade off PM/NO<sub>x</sub> is present. In fact, it is possible to see that increasing the EGR rate means to increase the emission of PM. It is interesting to see that for the tests conducted at 2250 rpm the curves with lower EGR rate have an higher formation peak with respect the ones with higher EGR rate, though the final value is lower. This could be justified by the higher temperature in the cylinder with lower EGR that promotes soot oxidation.

For all working conditions the soot process is not so influenced in the premixed phase, because the decrease of the oxygen concentration is more or less balanced by the longer ignition delay that promotes mixing.

Now a comparison between the use of the two fuels is done for each working point:

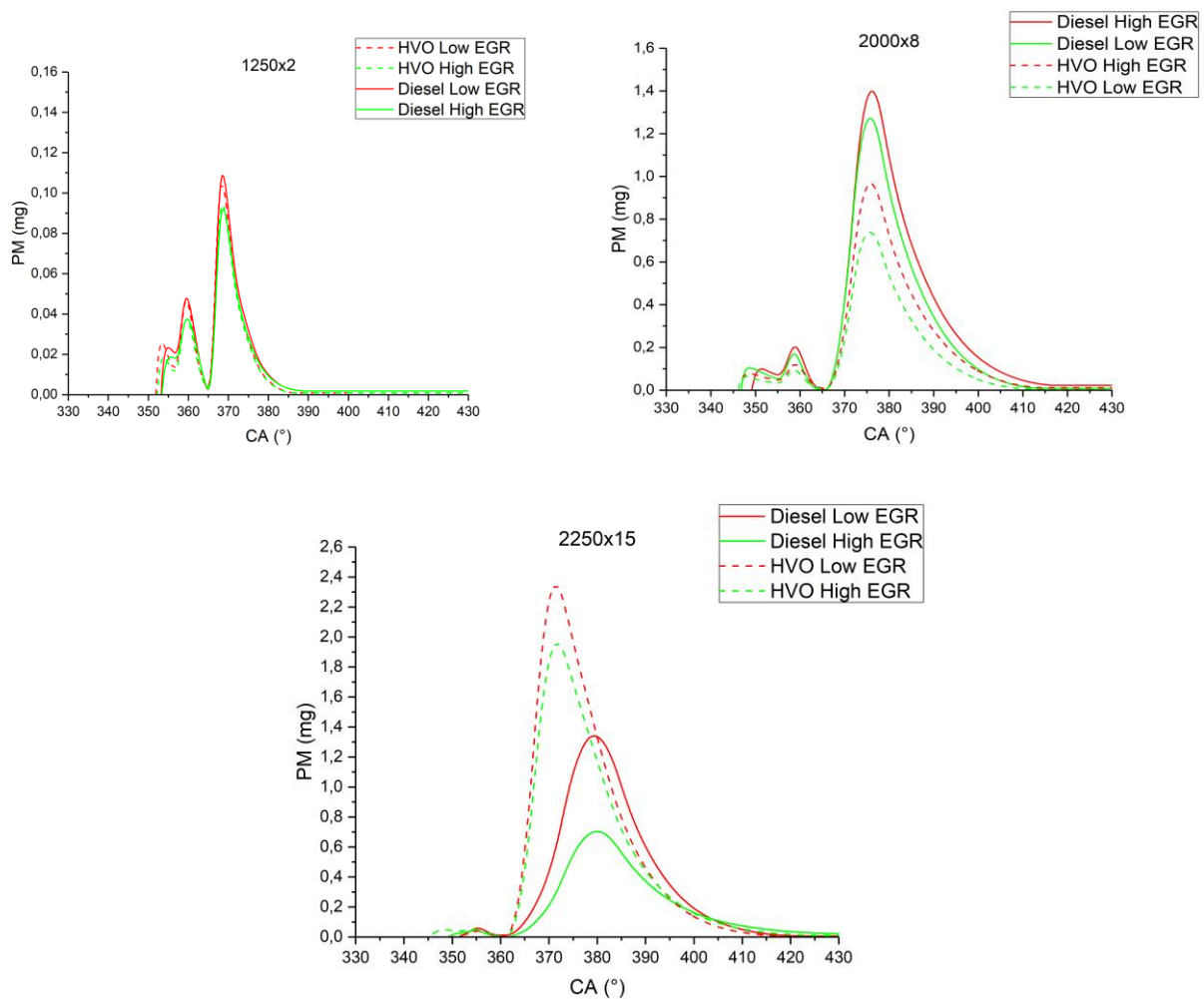


Figure 6.2 PM emission comparison between the two fuels

Those trends show that the tests performed with HVO as fuels have lower soot emission with respect the diesel one.

## 7. Conclusions

The aim of this thesis work was to refine an existing Matlab tool for the combustion and pollutant emission analysis of a CI engine in order to adapt it to another engine (the engine used is the F1A) and to investigate the behaviour of some parameters using two different type of fuel: conventional diesel and HVO.

The most important results are listed below:

- According to the three zone model, the fuel mass is underestimated for all tests and the model adds a certain quantity of fuel in order to calibrate the Woschni model;
- The comparison between the one zone model and the three zone one shows a faster heat release of the three zone model until the peak of the heat release rate. Then the one zone model has a faster heat release during the diffusive phase;
- The comparison between diesel tests and HVO ones shows that HVO develops higher burned zone temperatures and lower ignition delay;
- The increase of the EGR rate has caused an increase of the ignition delay, a decrease of the heat release rate peaks, a stretch of the combustion process and a decrease of the burned zone temperature;
- The nitrogen oxides concentration decreases if the EGR rate increases and higher EGR rate are needed at low load since exhaust gases are plenty of oxygen;
- The concentration of nitrogen oxides remains unchanged starting from 40° aTDC, where temperature in the burned gas zone starts to be lower than 2000 K;
- Compare nitrogen oxides emission for diesel and HVO did not show an unique trend for what type of fuel is better for NO<sub>x</sub> emission
- Low load working points have a behaviour similar to PCCI engines, where the trade-off between soot and nitrogen oxides is not present;
- HVO tests show lower soot emission with respect diesel ones

## ***Bibliography***

- [1] Stefano D'Ambrosio, *Combustion engines and their application to vehicle* (course material)
- [2] Ezio Spessa, *Design of engine and control systems* (course material)
- [3] Federico Millo, *Engine emission control* (course material)
- [4] John E. Dec, *SAE Technical Paper Series - A Conceptual Model of DI Diesel Combustion Based on Laser-Sheet Imaging*
- [5] Karavalakis, G., Jiang, Y., Yang, J., Durbin, T. et al., *Emissions and Fuel Economy Evaluation from Two Current Technology Heavy-Duty Trucks Operated on HVO and FAME Blends*
- [6] Bohl T., Smallbone A., Tian G., Roskilly A., *Particulate number and NOx trade-off comparisons between HVO and mineral diesel in HD applications*
- [7] J.B. Heywood, *Internal combustion engines fundamental*
- [8] Cristiana Delprete, *Powertrain components design* (course material)
- [9] G. Woschni, *A Universally Applicable Equation for the Instantaneous Heat transfer Coefficient in the Internal Combustion Engine*
- [10] Salvatore Frisulli, *Sviluppo di un tool diagnostico zero-dimensionale in ambiente Matlab per l'analisi della combustione e delle emissioni inquinanti in motori diesel*
- [11] R. Finesso, E. Spessa, *A real time zero-dimensional diagnostic model for the calculation of in cylinder temperatures, HRR and nitrogen oxides in diesel engines*
- [12] D. Jung, D.N. Assanis, *Quasidimensional Modeling of Direct Injection Diesel Engine Nitric Oxide, Soot, and Unburned Hydrocarbon Emissions*
- [13] A.E. Catania, S. D'Ambrosio, R. Finesso, E. Spessa, *Effects of Rail Pressure, Pilot Scheduling and EGR Rate on Combustion and Emissions in Conventional and PCCI Diesel Engines*